CMB Data Analysis:

1. Systematic effects of Beam Asymmetry: Effective Beams

2. Noise in Planck Sky Maps

K.M. Gorski

Sanjit Mitra, Graca Rocha

JPL/Caltech

Azores School on Observational Cosmology • Sept. 2011

Planck Effective Beams

Systematic Effects: Beam

- Planck will reach high accuracy goals, provided all the systematic effects are taken into account

- Beam is one of the most important sources of systematic effects, because:

$$\Delta T^{\mathrm{obs}}(\hat{\mathbf{q}}) = \int_{4\pi} \mathrm{d}\Omega_{\hat{\mathbf{q}}'} \, B(\hat{\mathbf{q}}, \hat{\mathbf{q}}') \, \Delta T(\hat{\mathbf{q}}') + n(\hat{\mathbf{q}})$$

beam

noise

  – map makers do not account for:
    - finite beam size
    - location of pointing within a pixel
  – observed CMB anisotropy sky is convolved with beam and scan

- Major tasks:
  – beam fitting & incorporating uncertainties in analyses
  – accounting for the effect of beam asymmetry

Planck Focal Plane & Scan

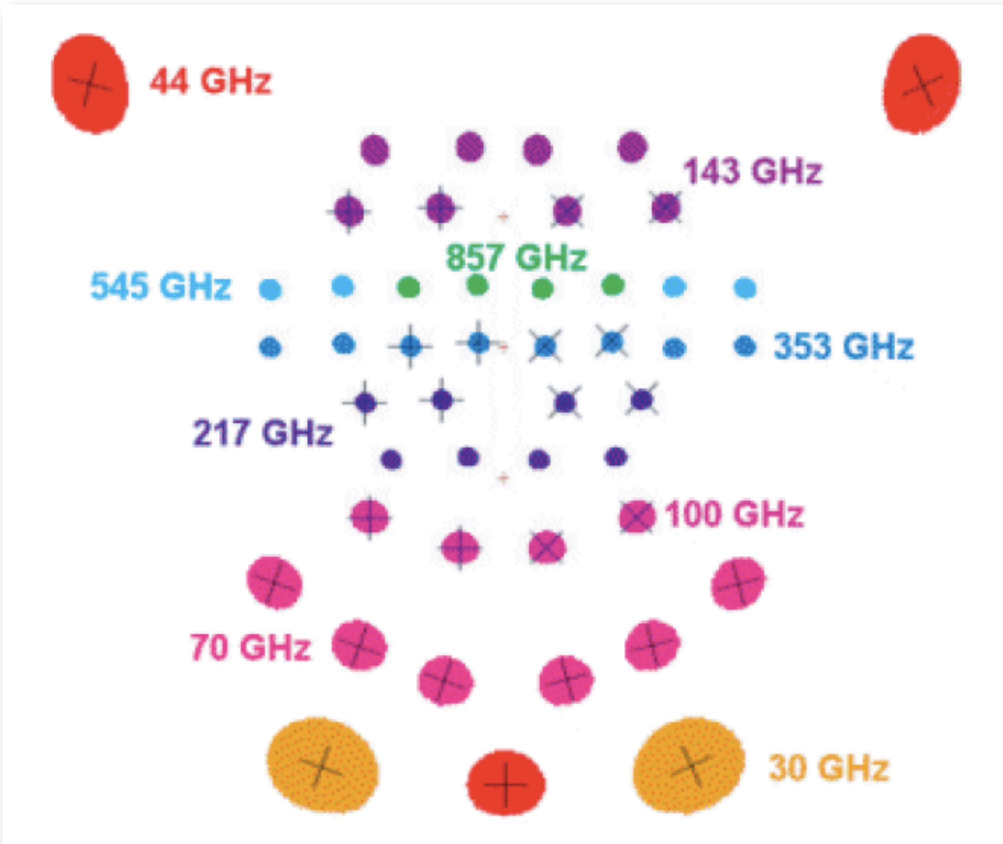

Main Beams on the Focal Plane

Planck Bluebook

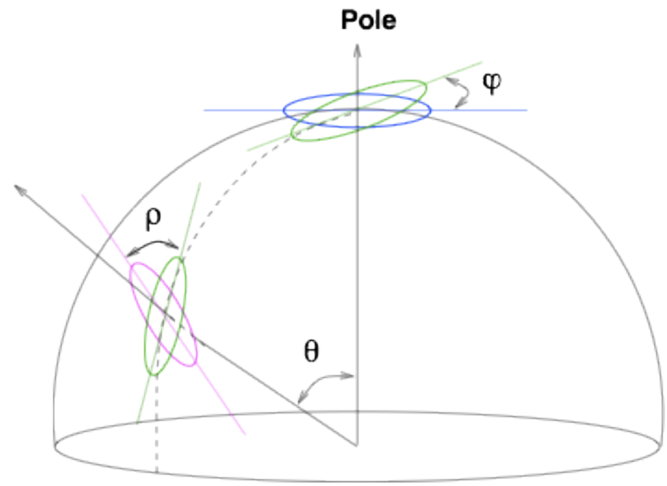

Beams rotate about the pointing direction

Planck Scanning Strategy –
Slow (6-months) Precession Case

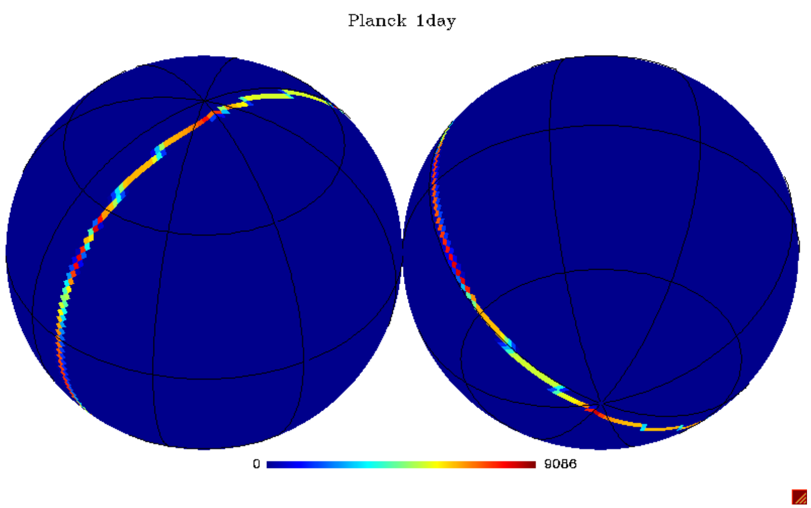

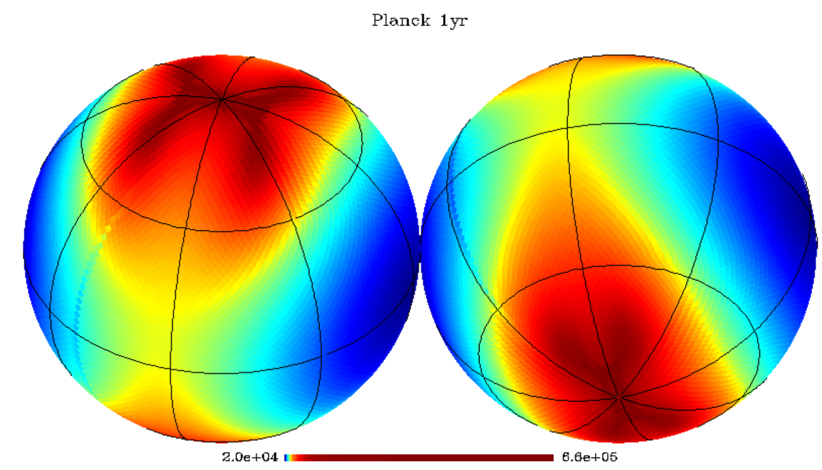

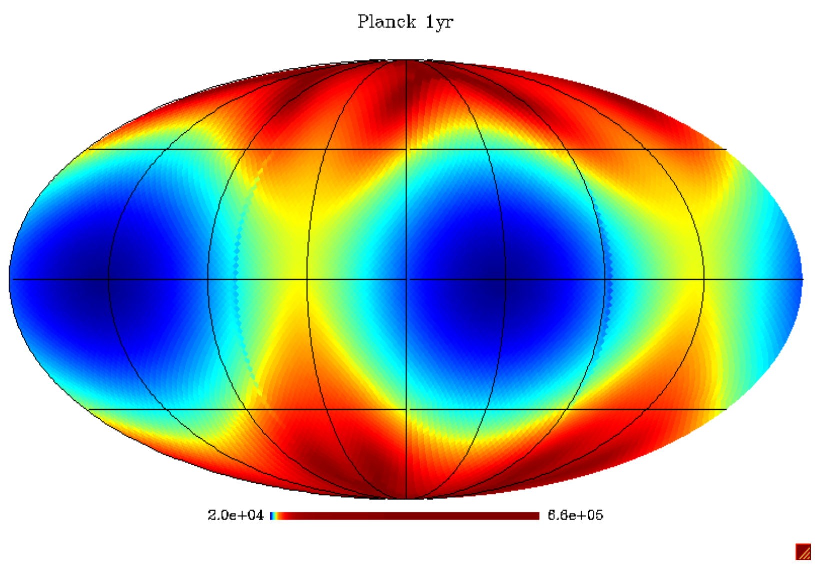

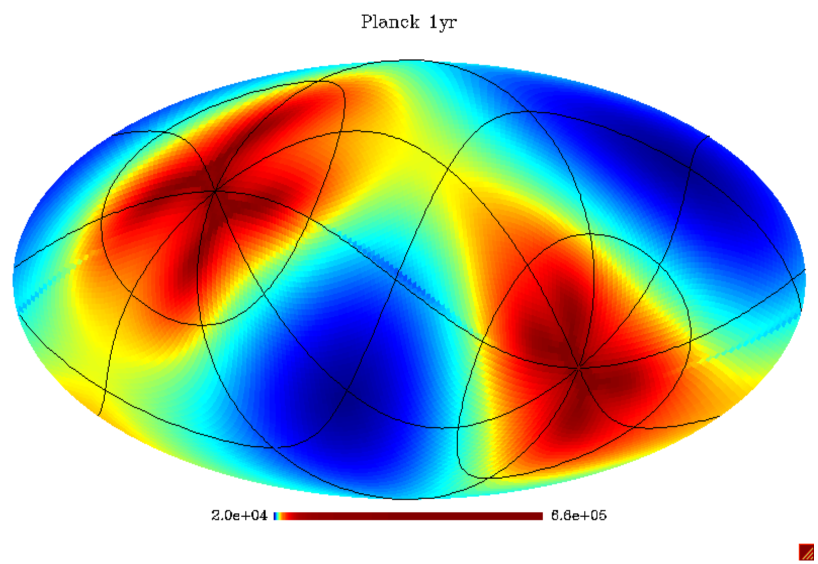

Forward (MC) Approach

- We take a forward MC route
  - find the beam transfer functions though simulations
  - correct the observed Pseudo-C_l accordingly

- Requires a fast convolution method, that can
  1. handle asymmetric beams
  2. include whole Planck scan strategy

Fast Convolution with Effective Beams

- Pixel based convolution is simple and fast
  - computation cost:

$$\sim N_{\text{beam}} N_{\text{pix}}$$

more complicated for polarization

- Effective beam: Sum of beams for all hits in a given pixel
- Observed pixelized sky map (map maker output) is a convolution of the true sky with the effective beams
- Effective beams are generally asymmetric
  - due to intrinsic asymmetry of the instrumental beams
  - hits distributions are not symmetric about pixel centers
- Effective beams vary across the sky
  - hits and pointing are distributed differently over different pixels

Mitra, Rocha, Gorski, Huffenberger, Eriksen, Ashdown & Lawrence (2010) ApJS, 193, 1, id.5

pixConv / effBeam

- **Pixel based convolution w/ effective beams**
  - pre-compute effective beams, may store on disk
  - convolve with pre-computed effective beams

- **Pipeline has been developed for Planck**
  - takes advantage of huge distributed computing resources at NERSC
  - codes/data delivered to Planck in DPCs

- **Very fast compared to previous methods, e.g., for 15 months of 30GHz (4 detectors)**
  - level-S takes few CPU hours per map
  - effective beam method takes few seconds per map!
    - (in addition to the pre-computation of effective beams)

Beam vs PSF

- **Angular response function of the instrument vs the image of a point source**
- **At the pole of HEALPix map**

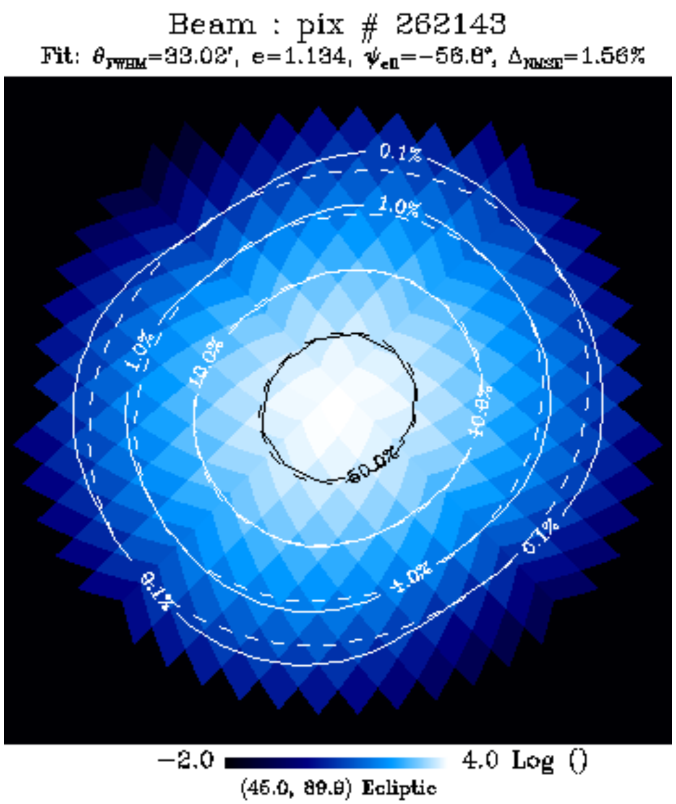

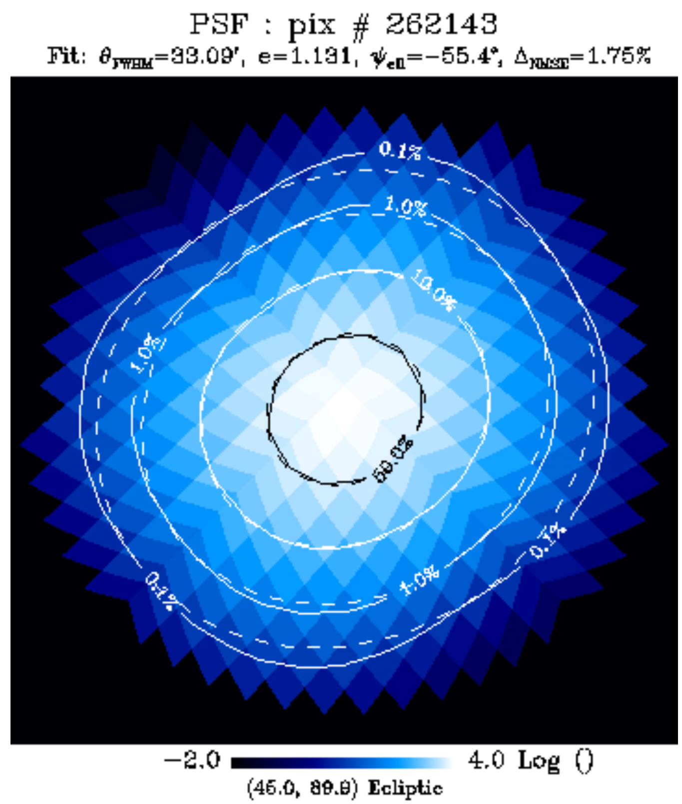

Beam

FWHM = 33.02’, e = 1.134, psi = -66.8

PSF

FWHM = 33.09’, e = 1.131, psi = -55.4

Beam vs PSF

- **At a cusp of Planck scanning strategy integrated count of observations**

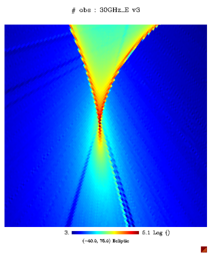

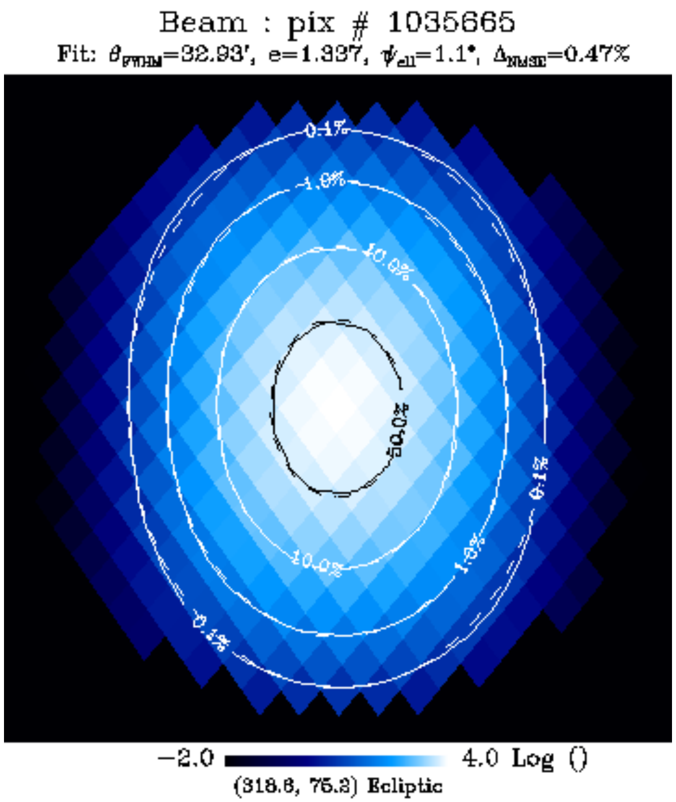

Beam

FWHM = 32.93’, e = 1.337, psi = 1.1

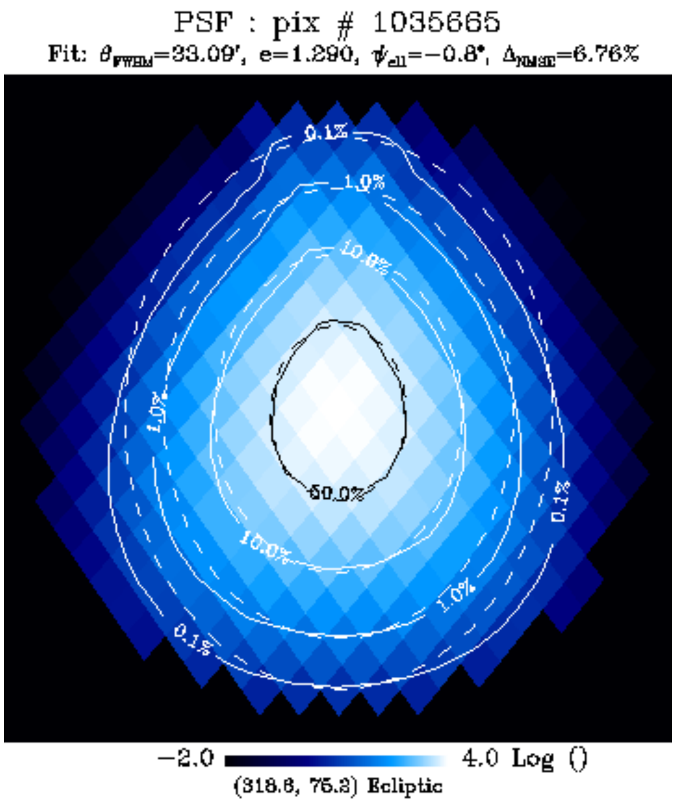

PSF

FWHM = 33.09’, e = 1.290, psi = -0.8

Beam vs PSF

- **At another cusp**

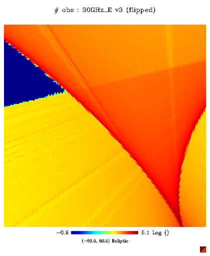

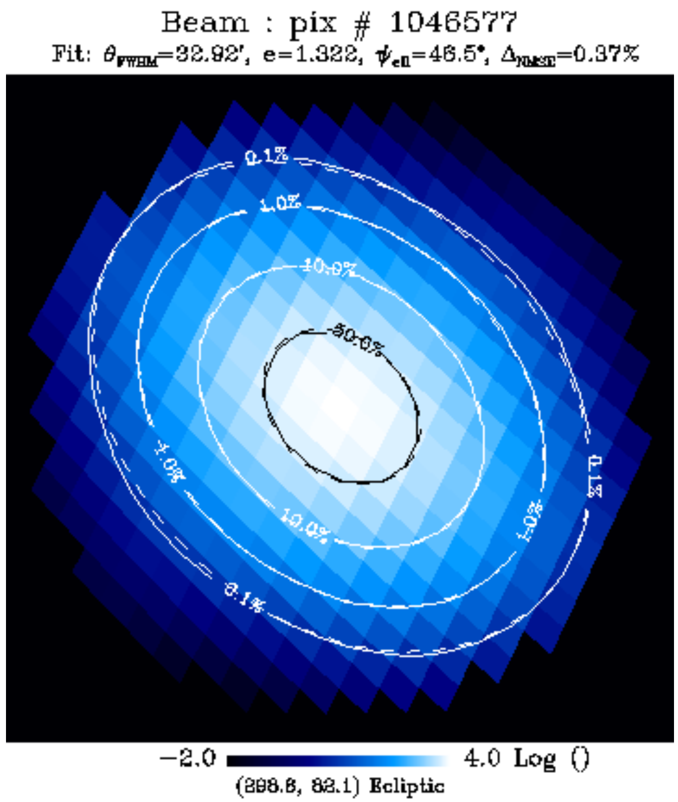

Beam

FWHM = 32.92’, e = 1.322, psi = -46.5

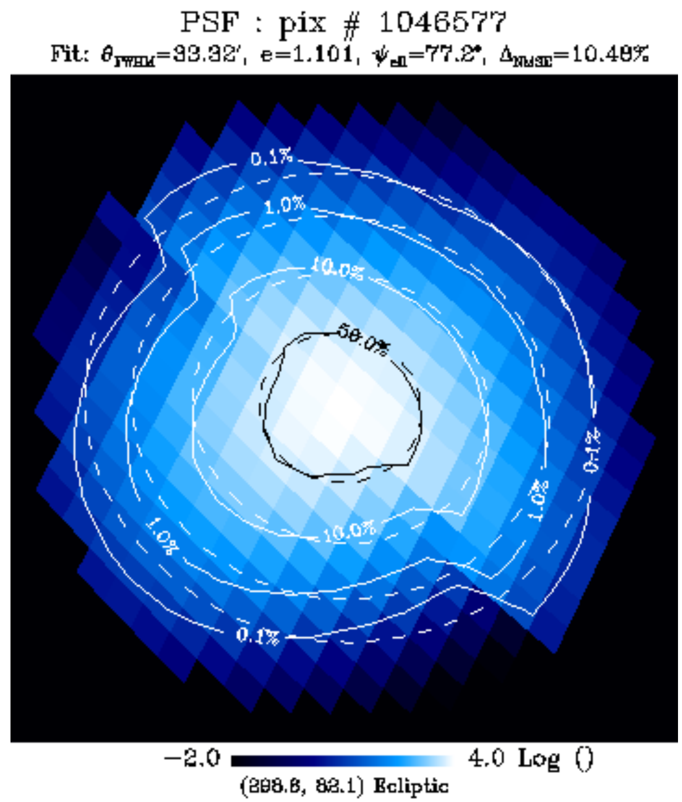

PSF

FWHM = 33.32’, e = 1.101, psi = 77.2

ERCSC Convolved Map

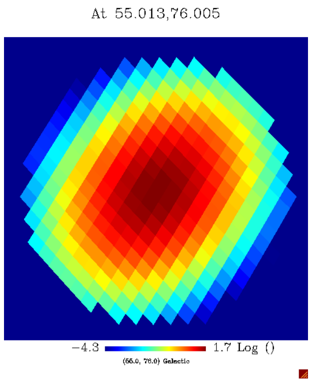

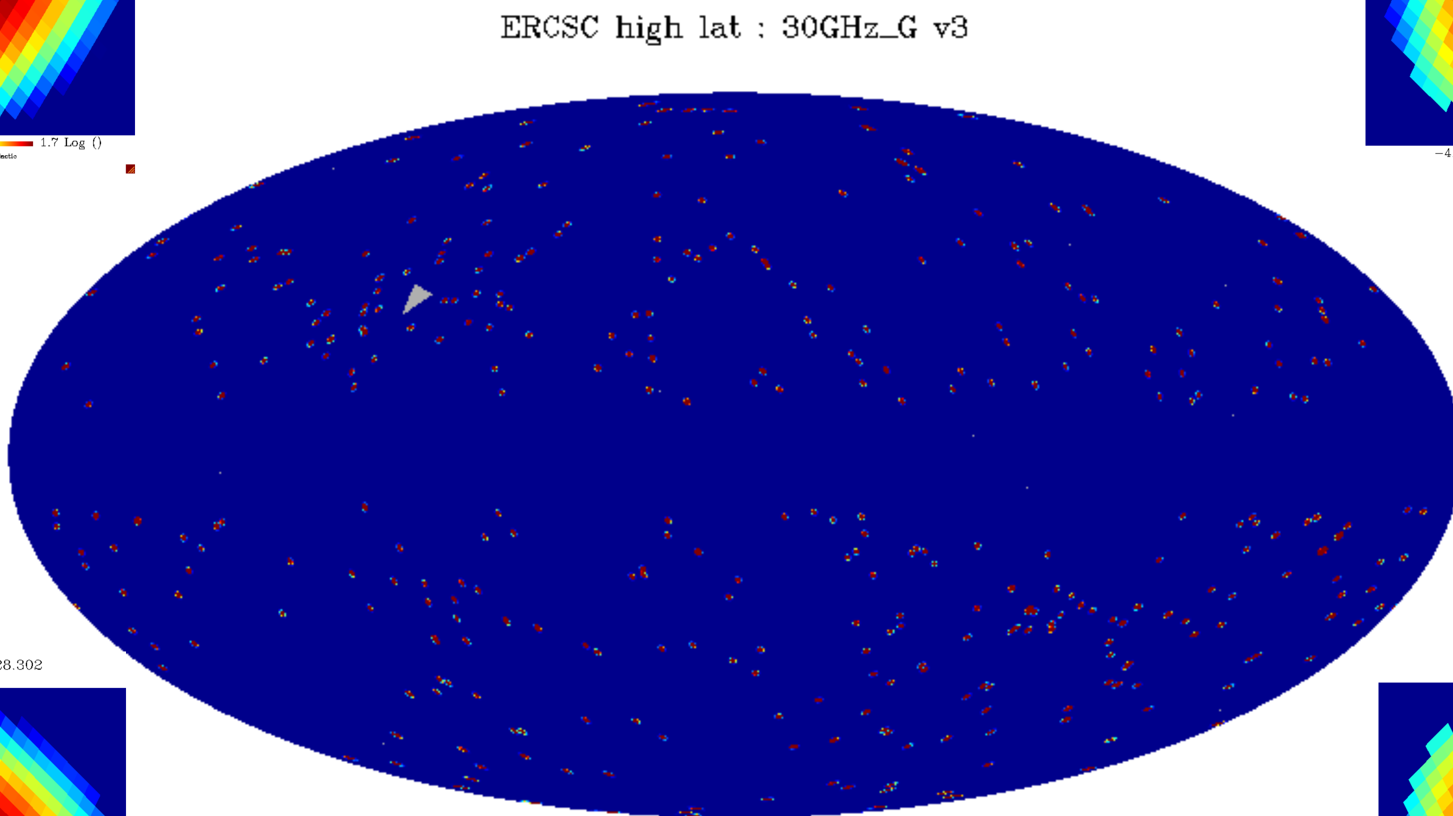

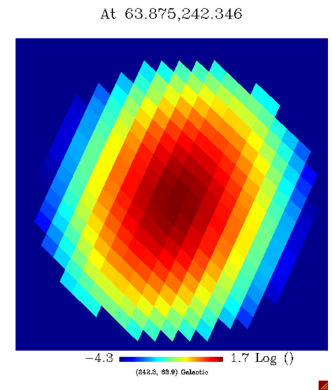

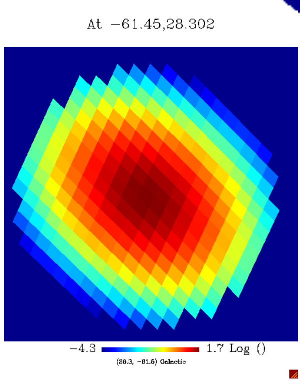

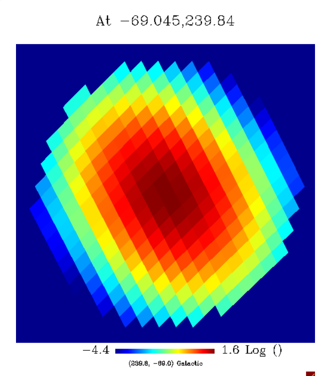

Planck ERCSC, one source position, 143 GHz

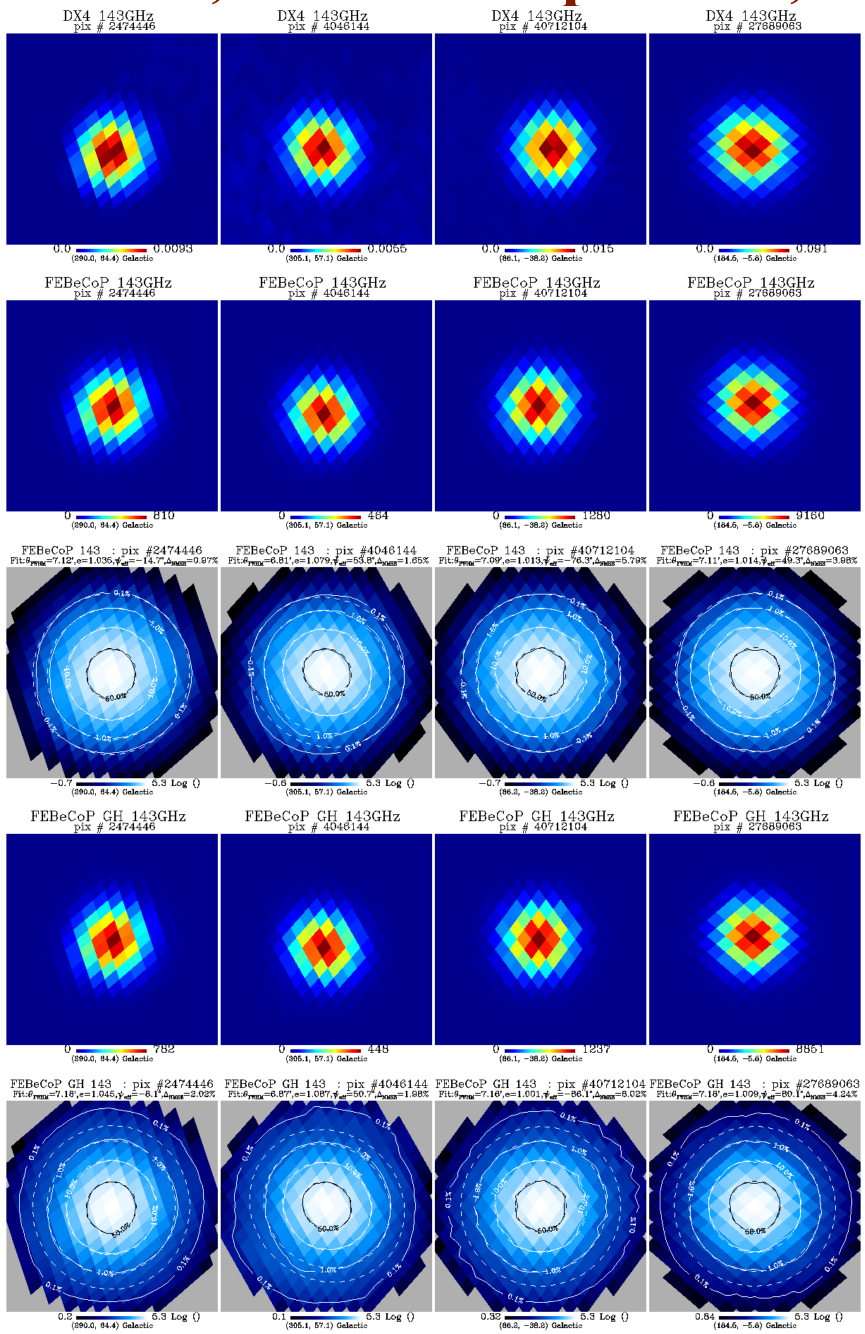

Image of an ERCSC object

FEBeCoP Input: Elliptical Gaussian fits of planet observations

FEBeCoP Input: Gauss-Hermite expansion based fits of planet observations

Shapes of ERCSC sources vs PSF from FEBeCoP

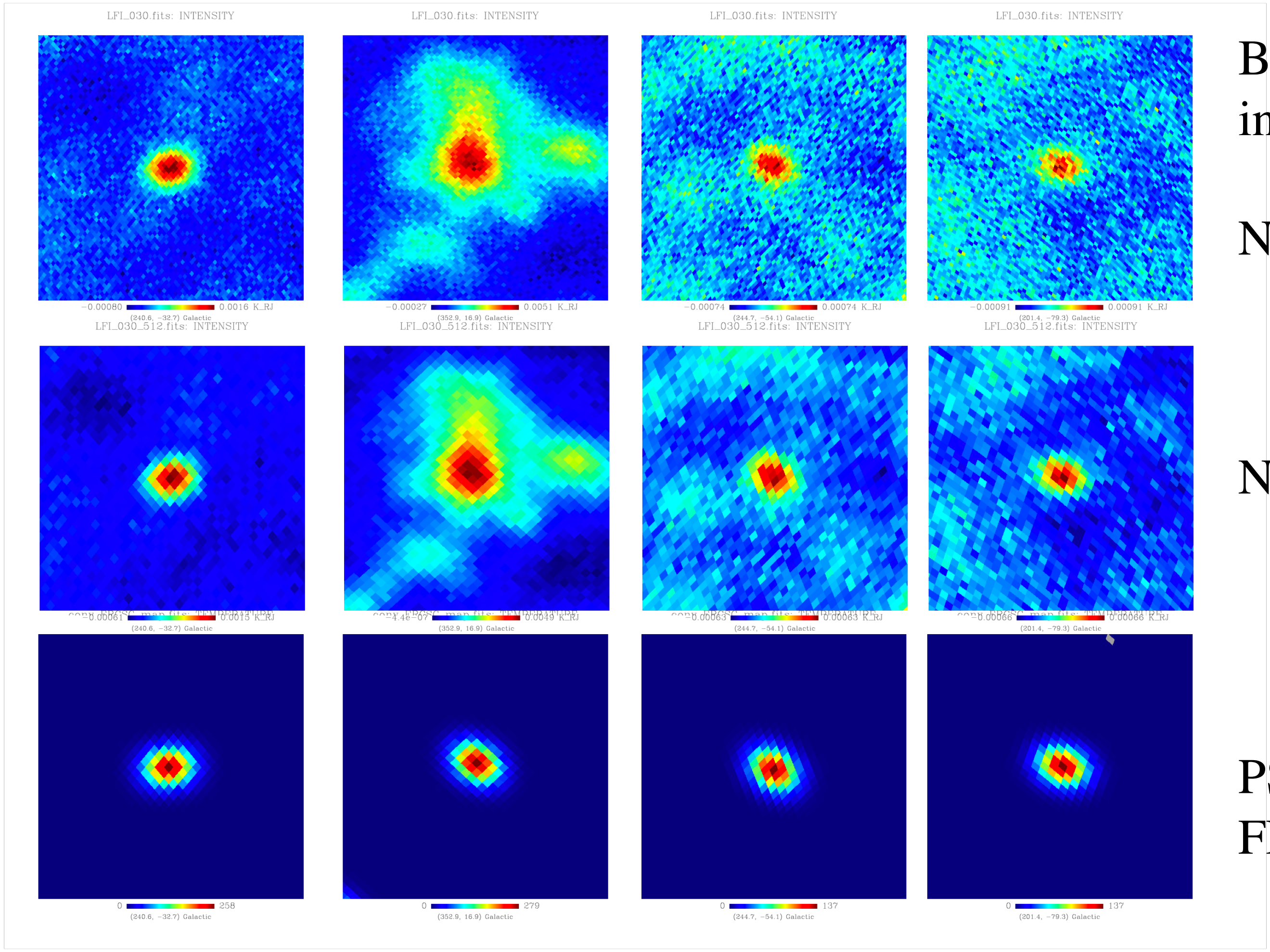

Bright sources
in ERCSC P3.0 cat

Nside=1024

Nside=512

PSF
FEBeCoP

Conclusion

- Planck promises extremely precise results
  - systematic effects must be accounted for to achieve that goal
- Beam asymmetry is a major source of systematic effect
  - specially for polarization
- We have developed a fast convolution pipeline
  - pixel based, pre-computes effective beams
- Current work: many simulations and ongoing study of systematic effects of beams and scanning in science oriented analyses

Noise in Planck Sky Maps

Assessing the Noise in the Planck Sky Maps - The Idea

- We take advantage of Planck scanning strategy by splitting TOI streams into two halves during each fixed pointing period
  - Nominally, this should result in re-observation of the same sky signals in both halves, and different noise streams
- We use such data sets to make separate (less sensitive) maps of the available time span of the mission
  - We have done this using all available map making codes
- Unless very long lag noise correlations (in excess of ~20 minutes) contribute significantly to Planck TOIs, the sum of such maps should equal that made out of the entire data set
- The difference map should inform us on the properties of the noise, especially its power spectrum, as for the noise the power spectra of the sum and difference maps should be identical (again, assuming small long lag noise correlations)
- Conversely: if the sum and difference maps render spectra that are different where noise dominates, we ought to think …

Integrated Observation Count

HFI Core Team: HFI Data Processing

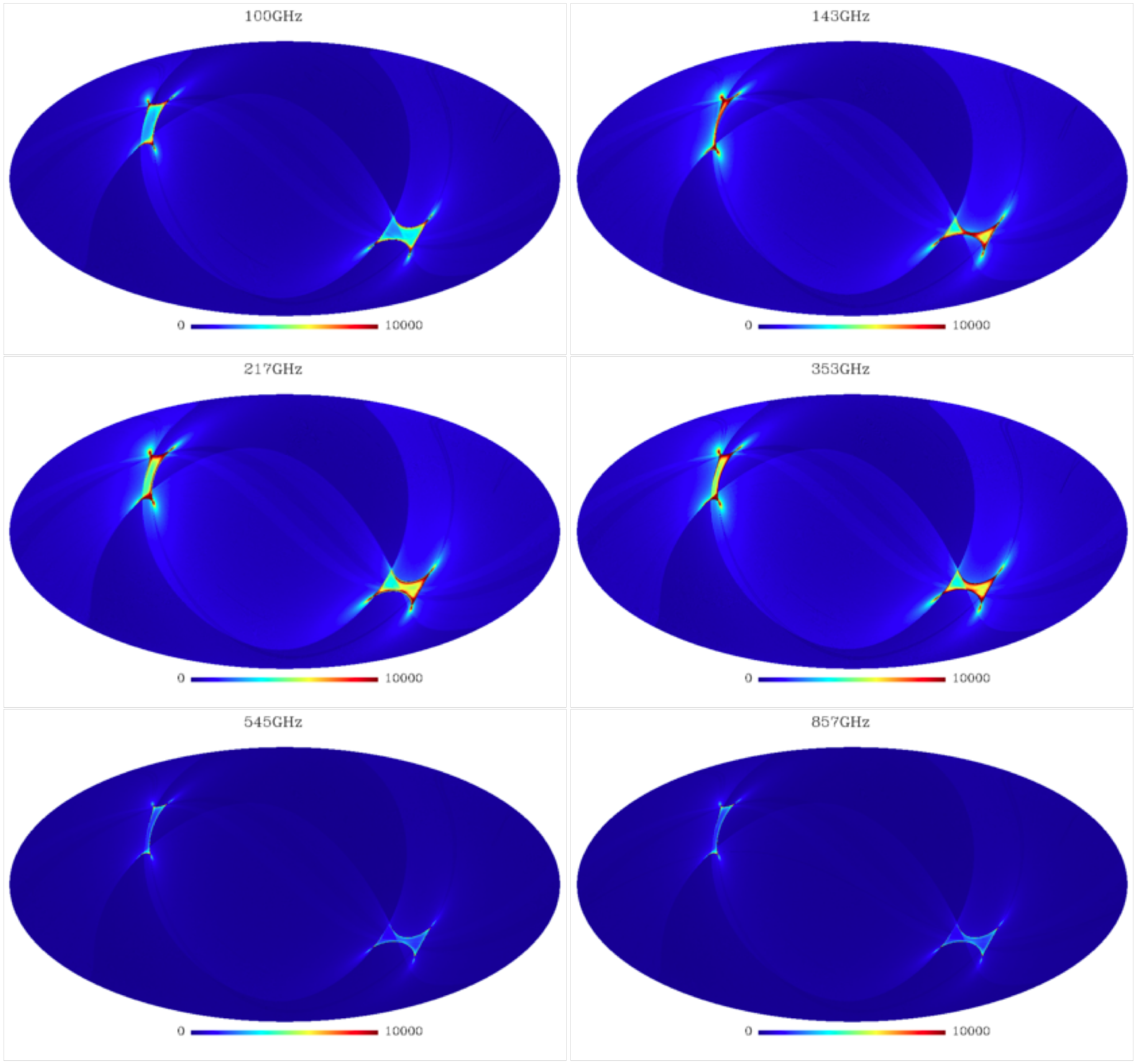

Figure 33. Hit count maps at each frequency (*from top left to bottom right :* 100, 143, 217, 353, 545, 857 GHz) in 1.7 arcmin pixels (Nside= 2048).

Noise in HFI Sky Maps

HFI Core Team: HFI Data Processing

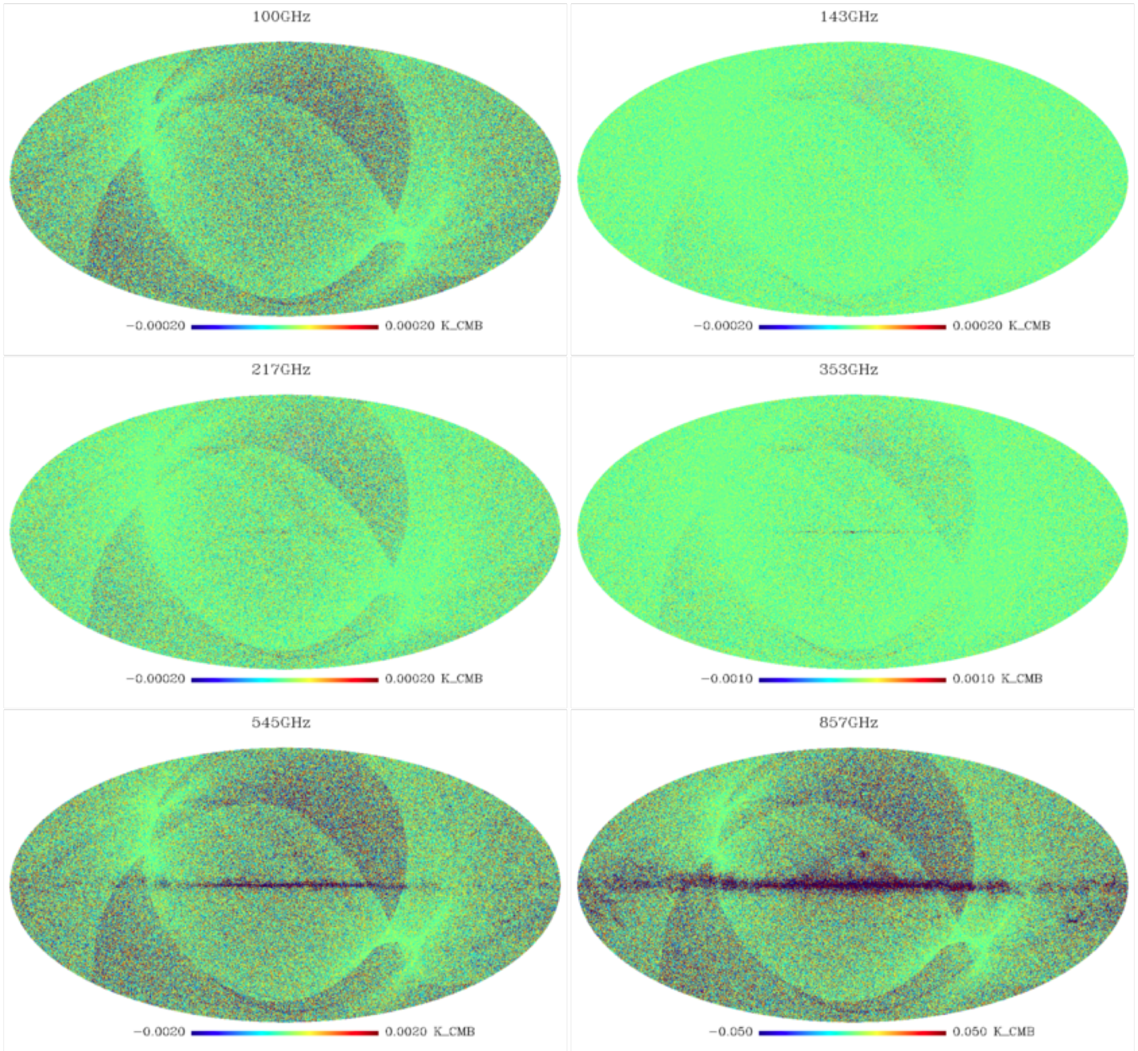

Figure 34. Residual maps of the half differences between the maps made from the first and second half rings projection (*from top left to bottom right:* 100, 143, 217, 353, 545, 857 GHz) in 1.7 arcmin pixels (Nside= 2048). Note that the CMB channels at 100-217 GHz are all shown on the same color scale. In addition the noise pattern, which is well traced by the hit maps of fig. 33, one also see the small differences (relative to the signal), when gradients of the signal are large (mostly in the Galactic plane) and sub-pixel effects become quite apparent.

Noise Power Spectra in the HFI Sky Maps

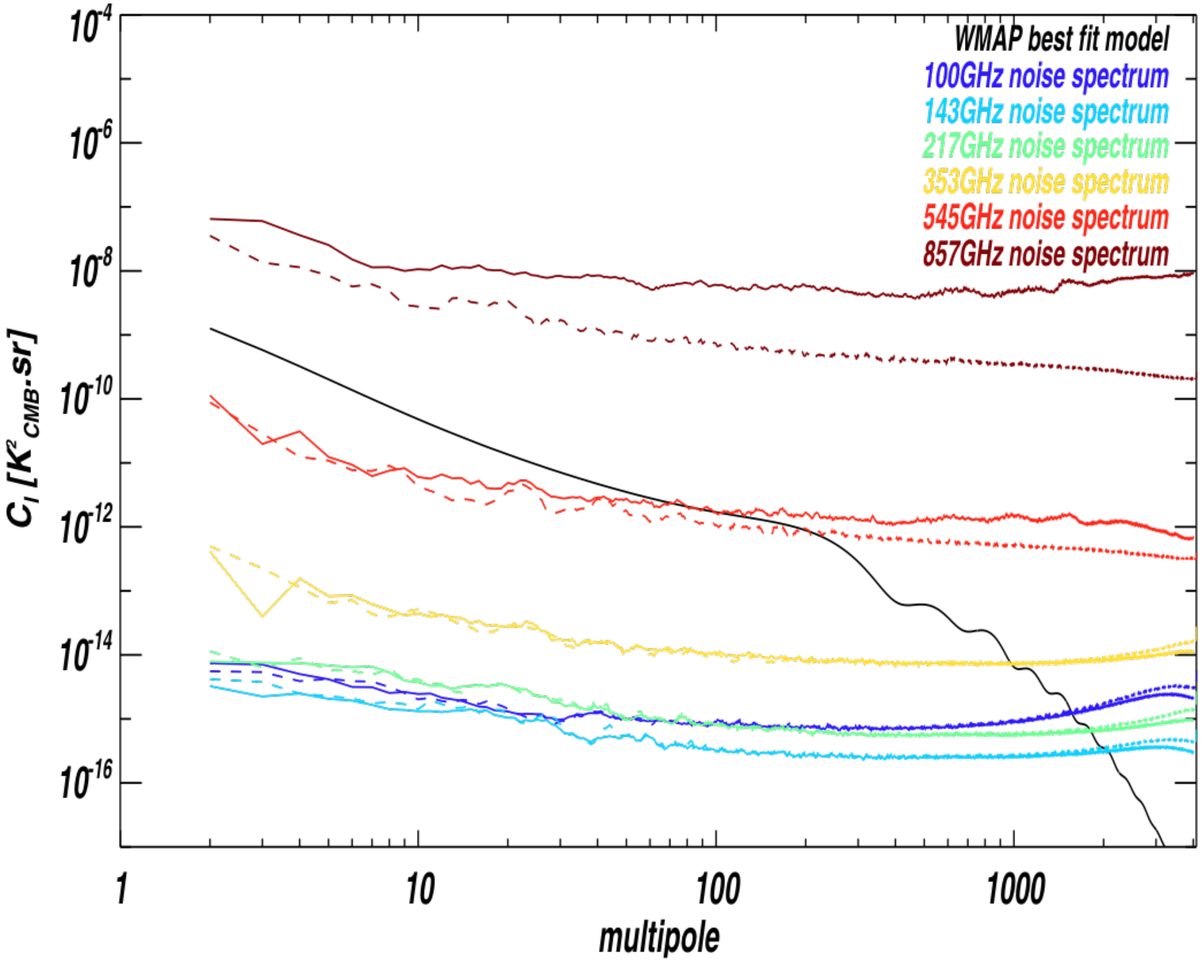

Figure 35. Power spectra from the difference maps shown on Fig. 34, on the full sky (*solid line*) and after masking the Galactic plane (*dashed line*). The sky coverage correction was done according to Tristram et al. (2005). As expected, the difference is only substantial at high frequency, when gradients of the Galactic signal are large.

Component Separation and CMB Reconstruction

Azores School on Observational Cosmology

Davide Pietrobon
in collaboration with **K.M. Górski**, J.G. Bartlett, L. Colombo,
J. Jewell, L. Pagano, **G. Rocha**, C.R. Lawrence & H.K. Eriksen

Outline

- Data Analysis in a nutshell
- Component Separation & Gibbs Sampling
- Example on WMAP
- Towards Planck
- Conclusions

Cosmic Microwave Background

1992

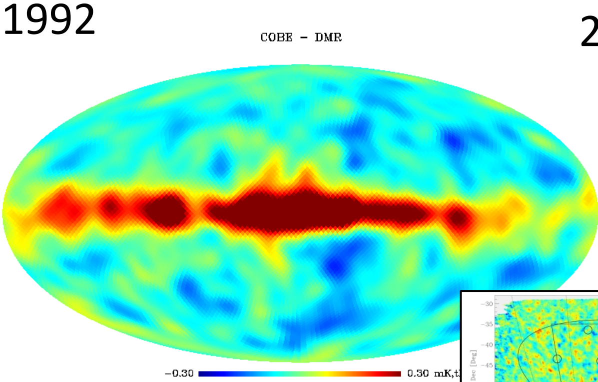

2003

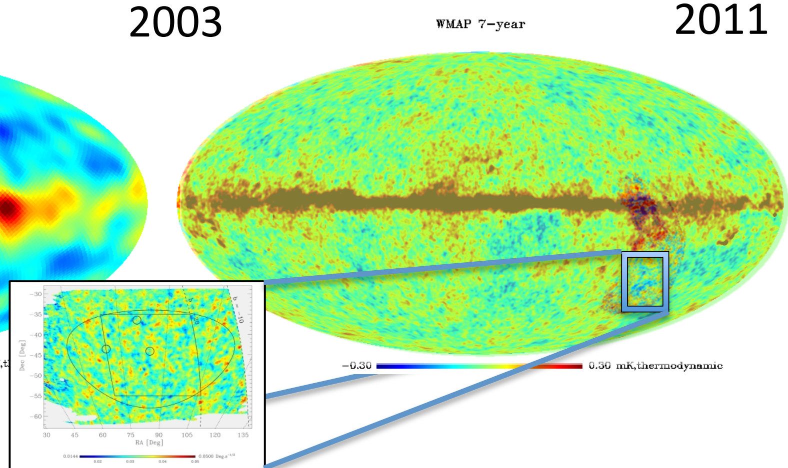

2011

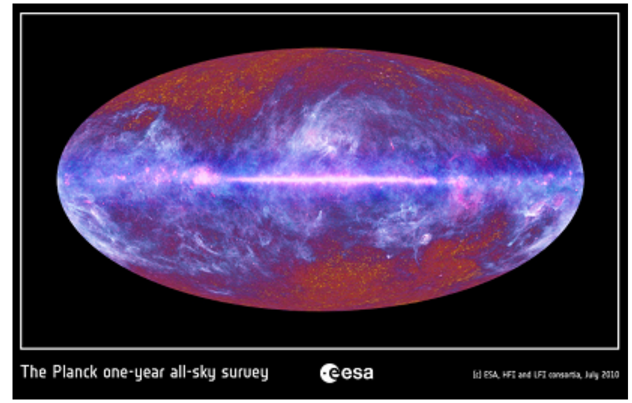

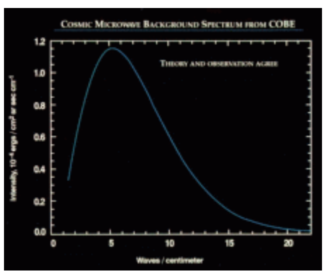

Black
body
spectrum
T=3μK

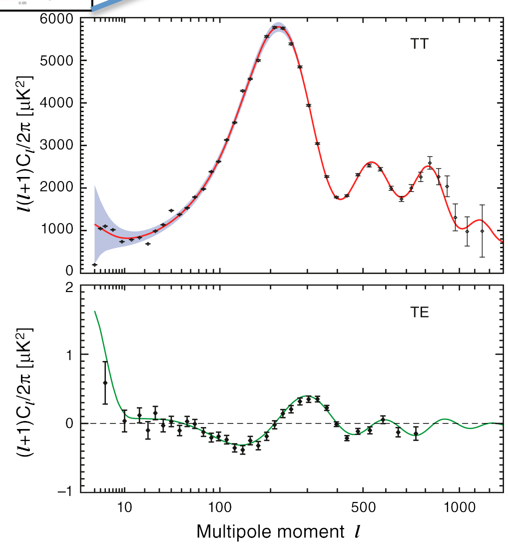

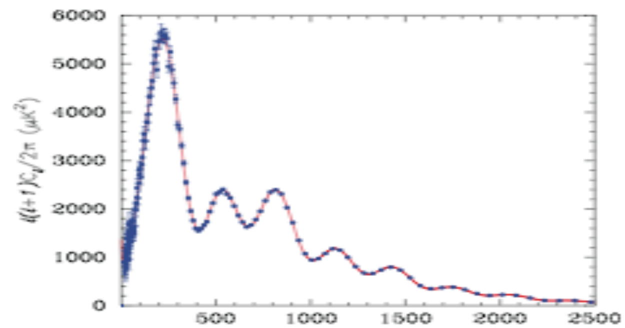

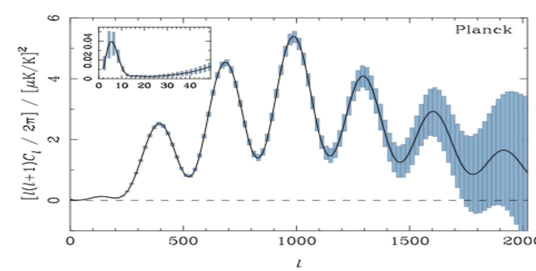

Sachs-
Wolfe
plateau
amplitude
$\delta T/T \approx 10^{-5}$

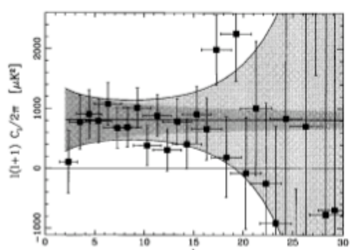

Flatness; matter content;
hint of coherent polarized signal

Cosmic variance limited; Early Universe physics; Polarization detection; reference for future surveys

CMB Data Analysis (1)

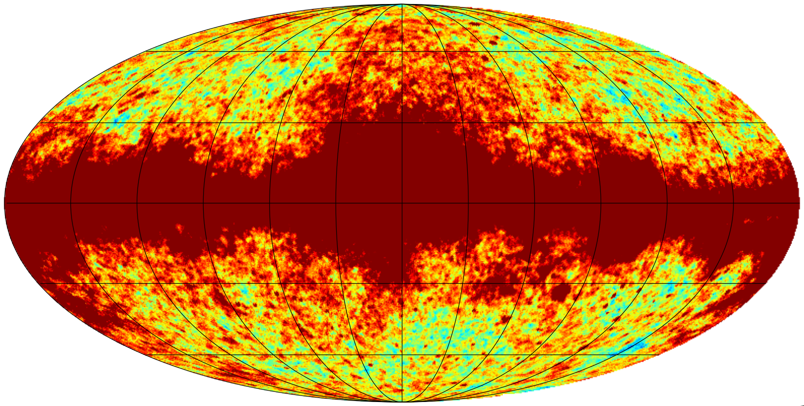

Wmap K-band

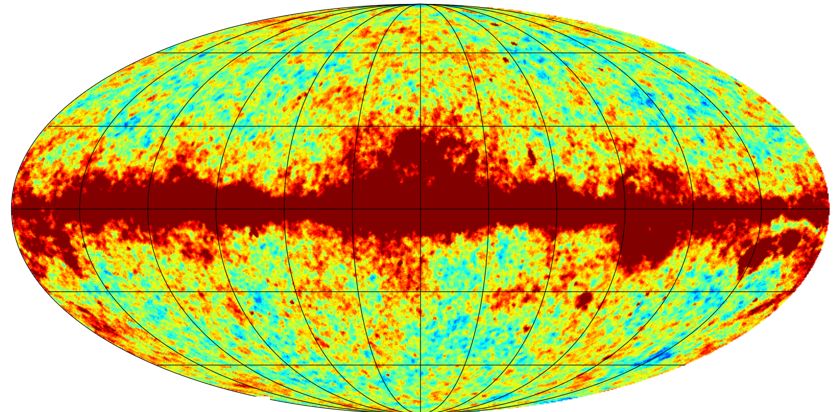

Wmap Ka-band

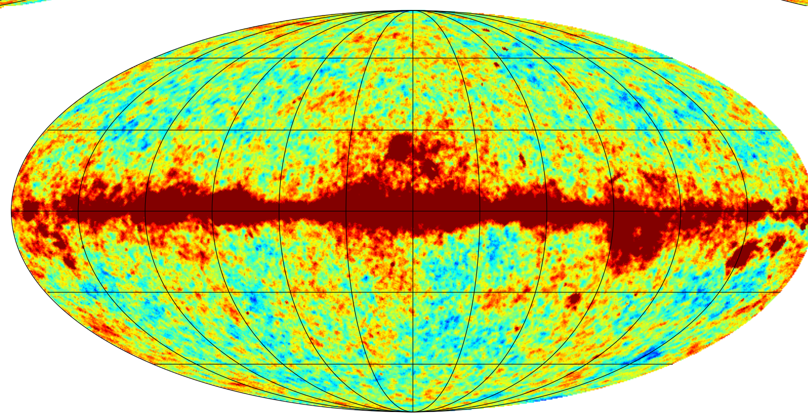

Wmap Q-band

Wmap V-band

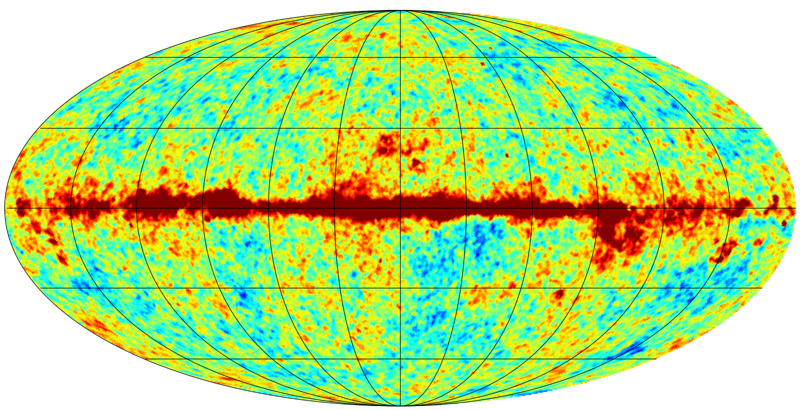

Wmap W-band

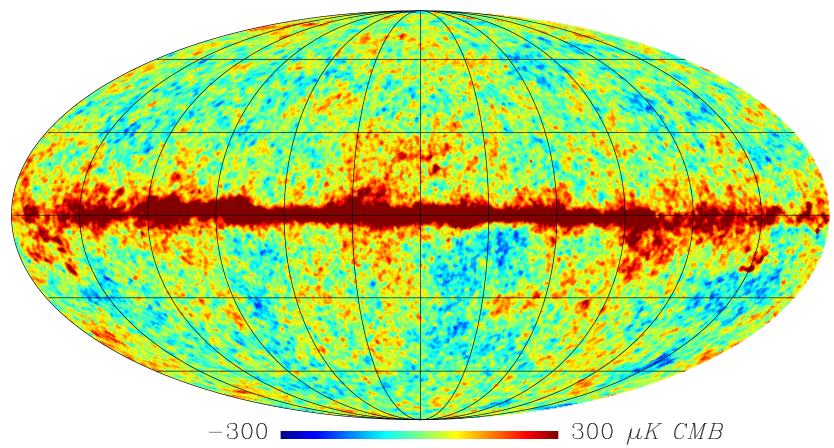

CMB Data Analysis (2)

Map: ~ 10^6 pixels

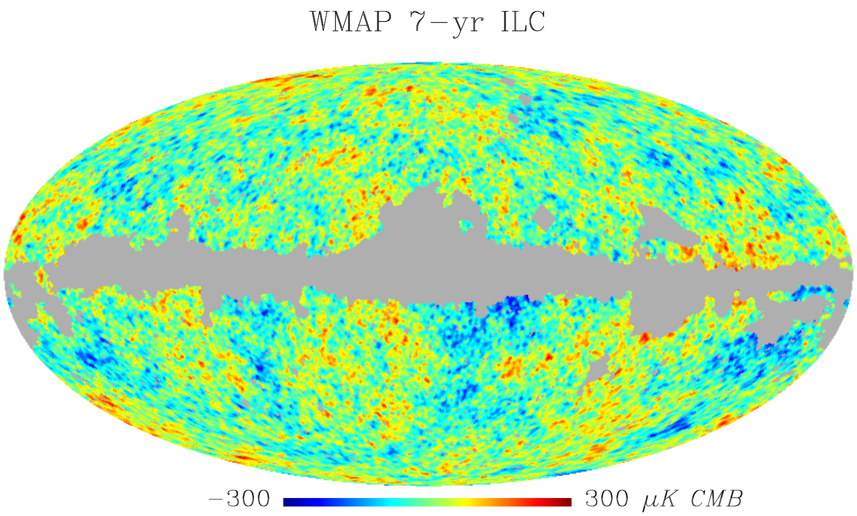

Isotropy

Angular Power Spectrum: ~ 10^3

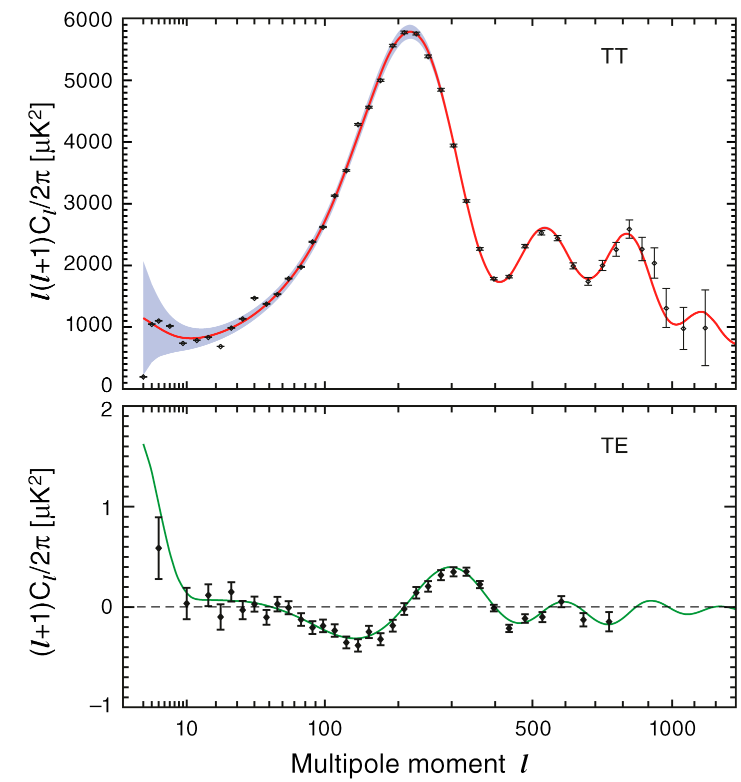

Parameters: ~ 10

$\Omega_b h^2$	$= 0.02267 \pm 0.00059$
$\Omega_c h^2$	$= 0.1131 \pm 0.0034$
Ω_Λ	$= 0.726 \pm 0.015$
n_s	$= 0.960 \pm 0.013$
$\Delta^2_{\mathcal{R}}$	$= (2.445 \pm 0.096) \times 10^{-9}$
τ	$= 0.084 \pm 0.016$
H_0	$70.5 \pm 1.3\, km\ s^{-1}$
Ω_b	0.0456 ± 0.0015
Ω_c	0.228 ± 0.013

Big data compression process!

Model fitting

Lots of Data are lost in process

- CMB:
  - Achieving the largest sky coverage possible;
  - Keeping information about the phases: CMB map;
- Foreground Study:
  - Distinguishing different physical components;
  - Studying their behaviour.

Commander

- Gibbs Sampler developed by B. Wandelt, J. Jewell, H. K. Eriksen @ JPL
  - Phys.Rev. D70 (2004) 083511 - **arXiv:astro-ph/0310080**;
  - Astrophys.J. 609 (2004) 1-14 - **arXiv:astro-ph/0209560**;
  - Astrophys.J.660:L81-L84,2007 - **arXiv:astro-ph/0701089**;
- CMB map, angular power spectrum;
- Foreground amplitudes and spectral indices;
- Posterior distribution: mean, variance, skewness, kurtosis;
- χ^2 as a measure of the goodness of the model;
- Relatively low resolution solution (CPU time!)

Gibbs Sampling (1)

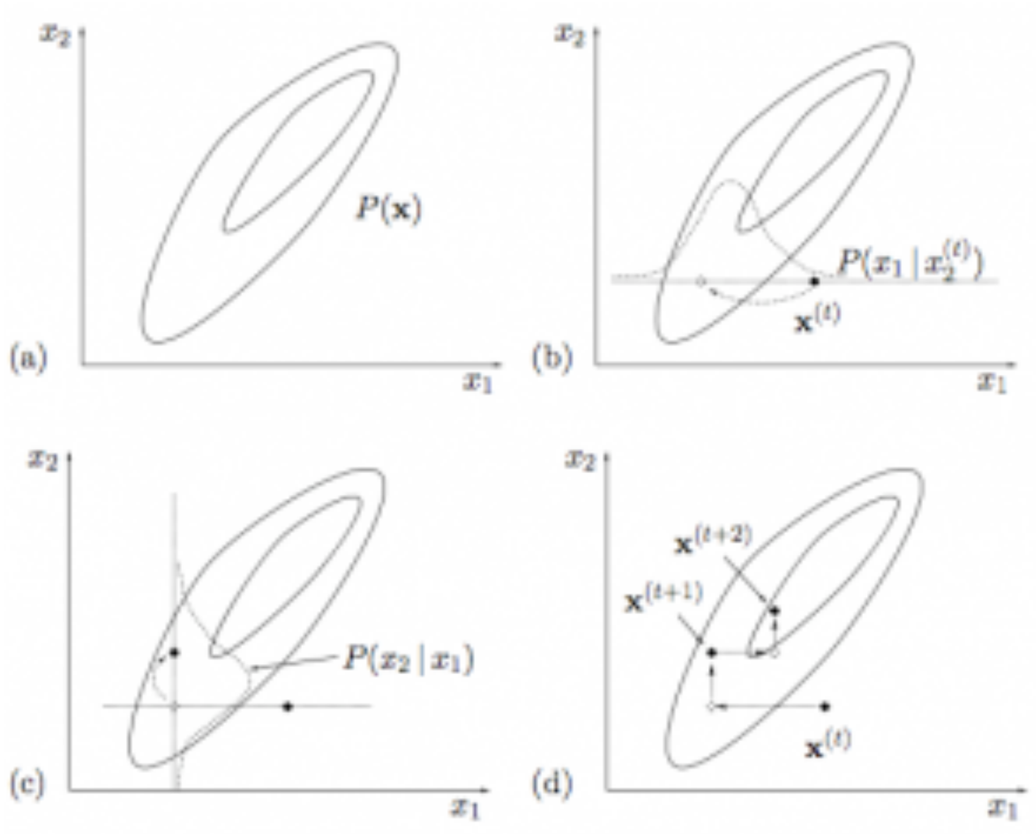

Bayes' Theorem:
Data, d
Theory, t

$$P(t|d) \propto P(d|t)P(t)$$

$$t = t(\theta_i, \theta_2, \ldots, \theta_i)$$

$$x_1 \rightarrow \mathrm{CMB}$$

$$x_2 \rightarrow \mathcal{C}_\ell$$

$$P(\mathbf{s}, C_\ell|\mathbf{d}) \propto P(\mathbf{d}|\mathbf{s}, C_\ell)P(\mathbf{s}, C_\ell)$$
$$\propto P(\mathbf{d}|\mathbf{s}, C_\ell)P(\mathbf{s}|C_\ell)P(C_\ell)$$

Gibbs Sampling (2)

$$P(\mathbf{s}, C_\ell|\mathbf{d}) \propto e^{-\frac{1}{2}(\mathbf{d}-\mathbf{s})^t\mathbf{N}^{-1}(\mathbf{d}-\mathbf{s})} \prod_\ell \frac{e^{-\frac{2\ell+1}{2}\frac{\sigma_\ell}{C_\ell}}}{C_\ell^{\frac{2\ell+1}{2}}} P(C_\ell)$$

$$\boxed{\mathbf{d}_\nu = \mathbf{A}_\nu \mathbf{s} + \sum_{k=1}^{K} \mathbf{c}_k \; \mathbf{g}_k(\nu;\theta_k) + \mathbf{n}_\nu}$$

$$\sigma_\ell = \frac{1}{2\ell+1}\sum_m |a_{\ell m}|^2$$

$$\{\mathbf{s}^{i+1}, \mathbf{c}_k\}^{i+1} \leftarrow P(\mathbf{s}, \mathbf{c}_k|C_\ell^i, \theta^i, \mathbf{d})$$

$$\theta^{i+1} \leftarrow P(\theta|C_\ell^i, \mathbf{s}^{i+1}, \mathbf{c}_k^{i+1}, \mathbf{d})$$

$$C_\ell^{i+1} \leftarrow P(C_\ell|\mathbf{s}^{i+1}, \mathbf{d}).$$

- Amplitudes: s(p), c_k(p)
- Foregrounds

Parameters: θ_k(p) (non linear)

- Power Spectrum: C_l

Foregrounds

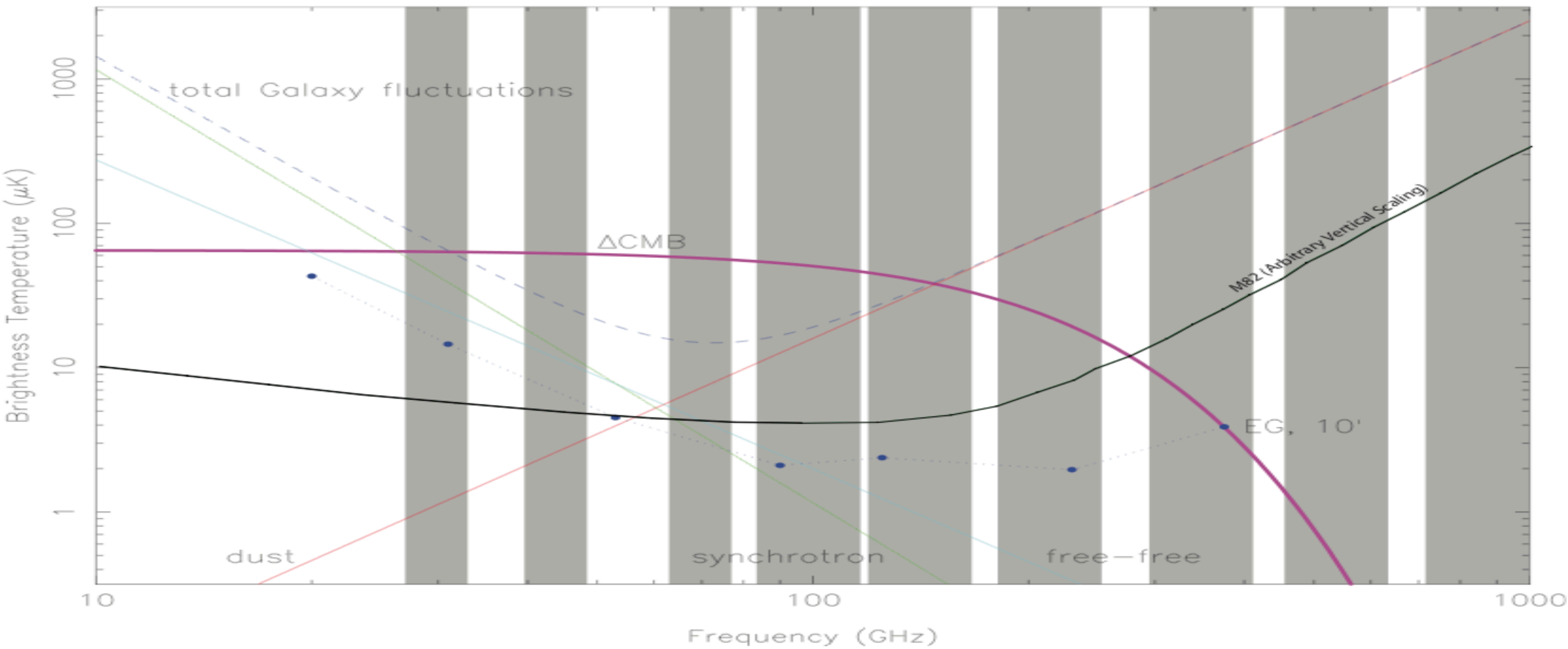

$$D(\nu) = A_d\Big(\frac{\nu}{\nu_d}\Big)^{\beta}\frac{B(\nu,T)}{B(\nu_d,T)}, \qquad \beta \simeq 1.6, T \simeq 18$$

$$S(\nu) = A_s\Big(\frac{\nu}{\nu_s}\Big)^{\alpha}, \qquad \alpha \simeq -3$$

$$f(\nu) = A_f\Big(\frac{\nu}{\nu_f}\Big)^{\epsilon}, \qquad \epsilon \simeq -2.15$$

WMAP 7-yr Data Processing

- 60 arcmin smoothing applied;
- Downgrade to N_{side}=128;
- White noise added from MC;
- C_l sampling on;
- Residual monopole and dipole fitted;
- Kq85 Galactic plane mask;
- Foreground model per pixel.

$$T_\nu(\hat{\gamma}) = B_\nu s(\hat{\gamma}) + N_\nu(\gamma) + M + D(\hat{\gamma}_0 \cdot \hat{\gamma}) +$$
$$A_d(\hat{\gamma})\left(\frac{\nu}{\nu_d}\right)^{\beta(\hat{\gamma})}\frac{B(\nu, T(\hat{\gamma}))}{B(\nu_d, T(\hat{\gamma}))} + A_s(\hat{\gamma})\left(\frac{\nu}{\nu_s}\right)^{\alpha(\hat{\gamma})} + A_f(\hat{\gamma})\left(\frac{\nu}{\nu_f}\right)^{\epsilon}$$

COMMANDER outputs

- few chains -> thousands of samples;
- C_l, CMB map, foreground model and χ^2 for every step;
- Mean CMB map, foreground amplitude and indices derived;
- Distribution of C_l computed: mode taken as most likely value;
- Error bars computed from 68% of the distribution;

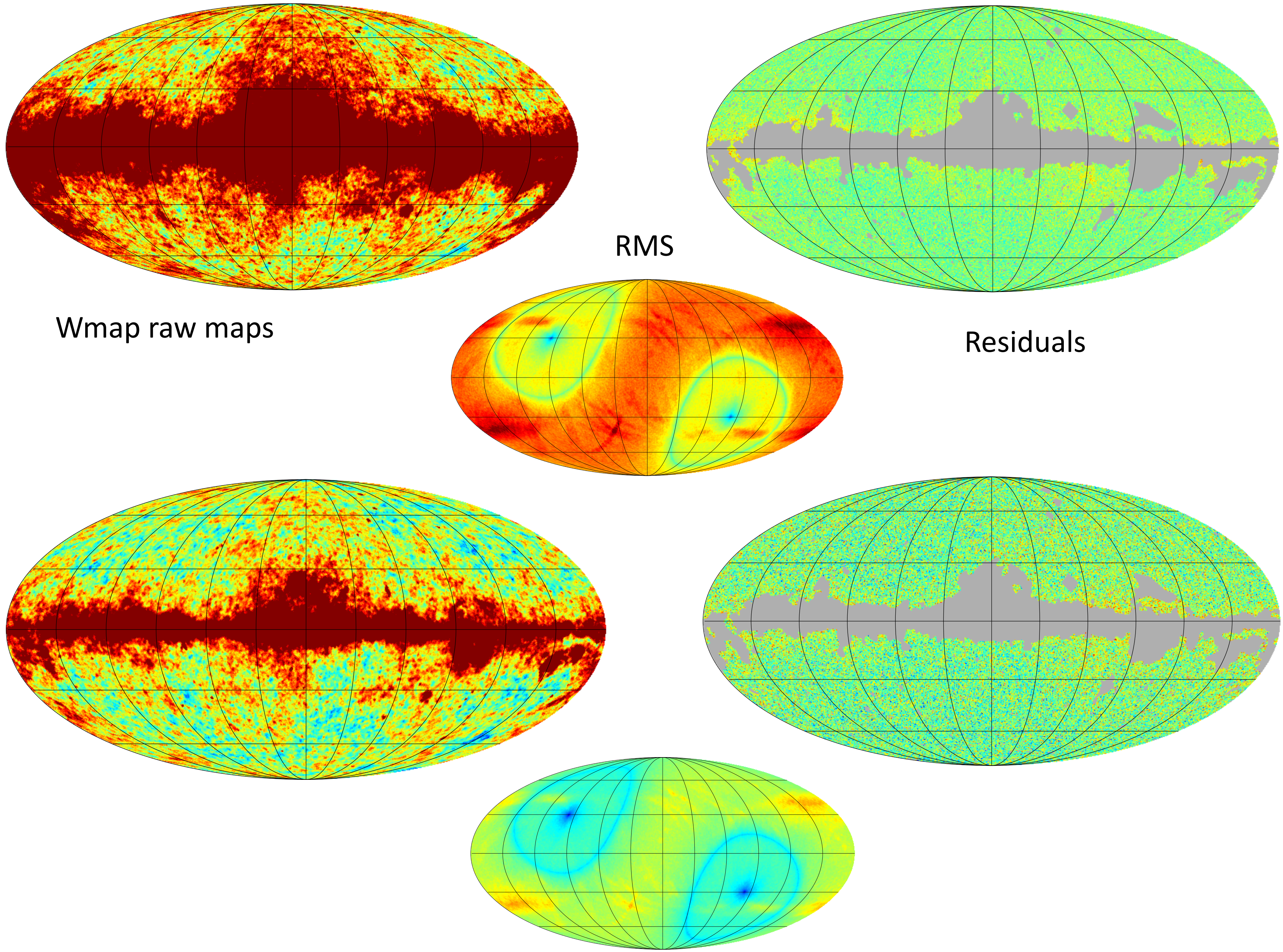
Wmap raw maps
RMS
Residuals

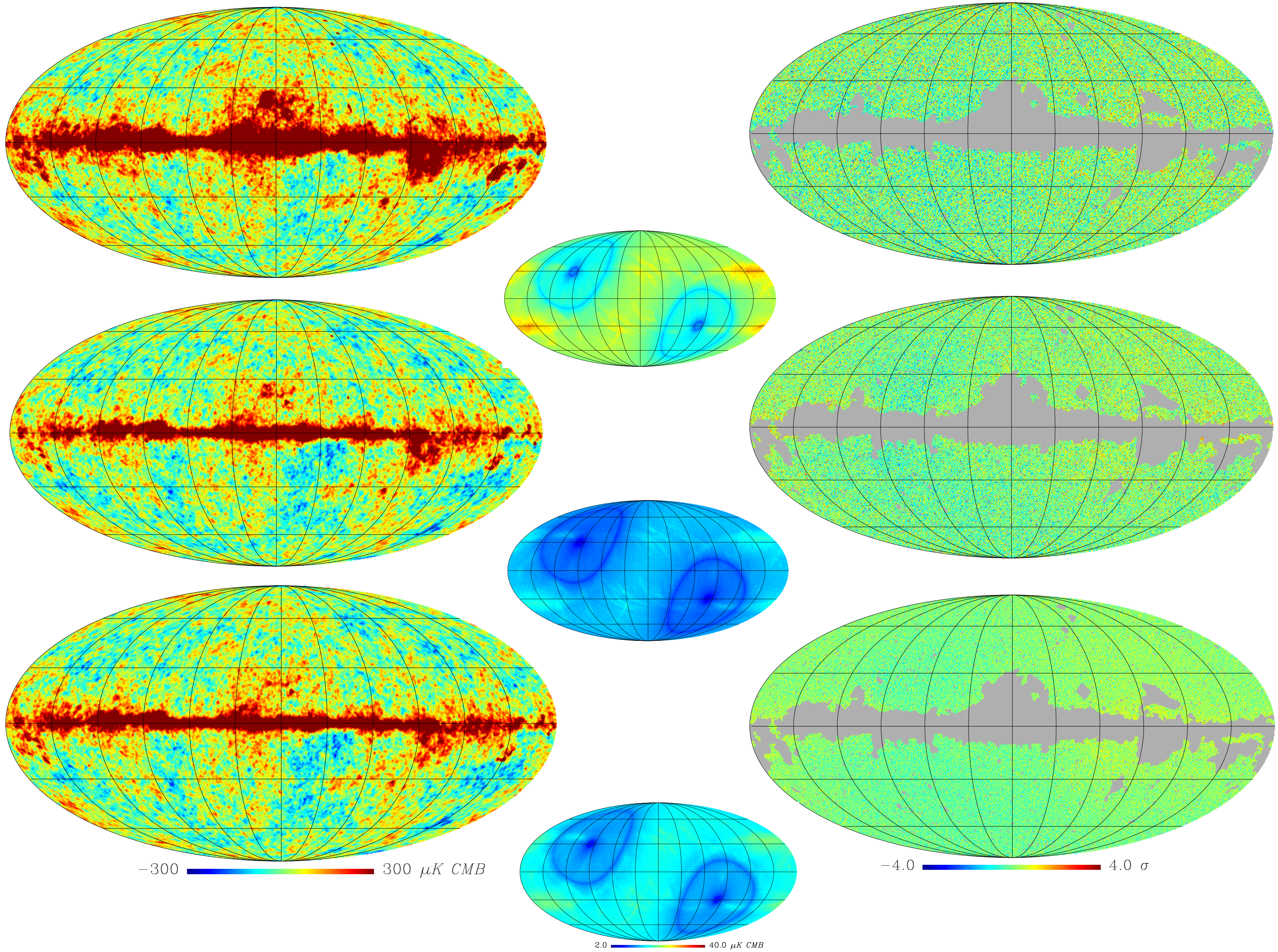

−300
300 μK CMB
2.0
40.0 μK CMB
−4.0
4.0 σ

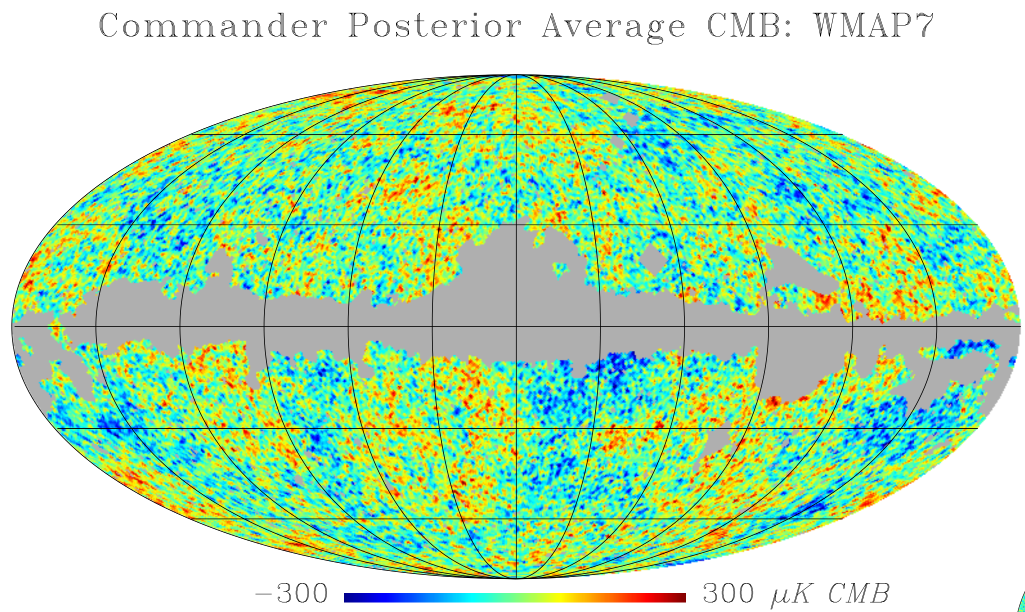
Commander Posterior Average CMB: WMAP7
−300
300 μK CMB

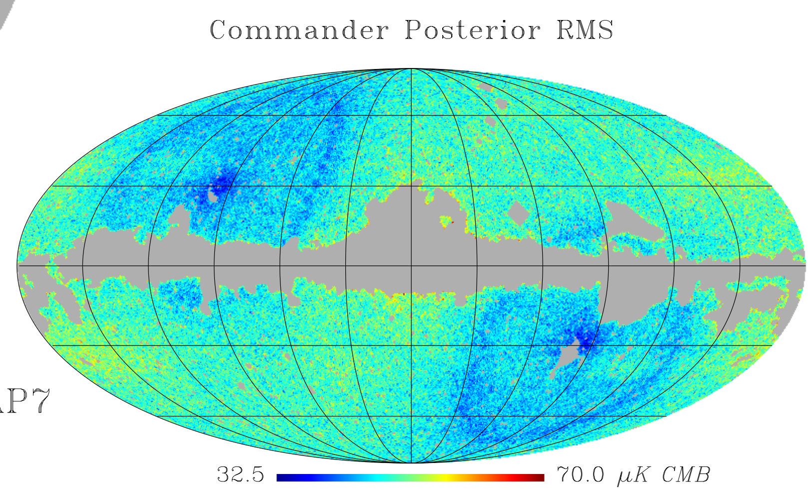
Commander Posterior RMS
32.5
70.0 μK CMB

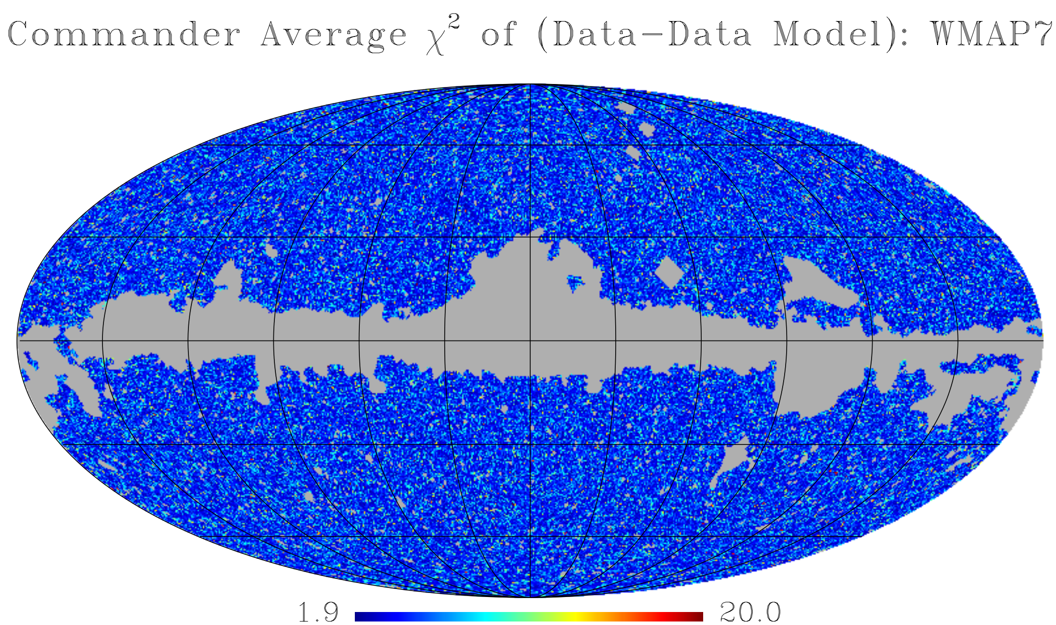
Commander Average χ^2 of (Data−Data Model): WMAP7
1.9
20.0

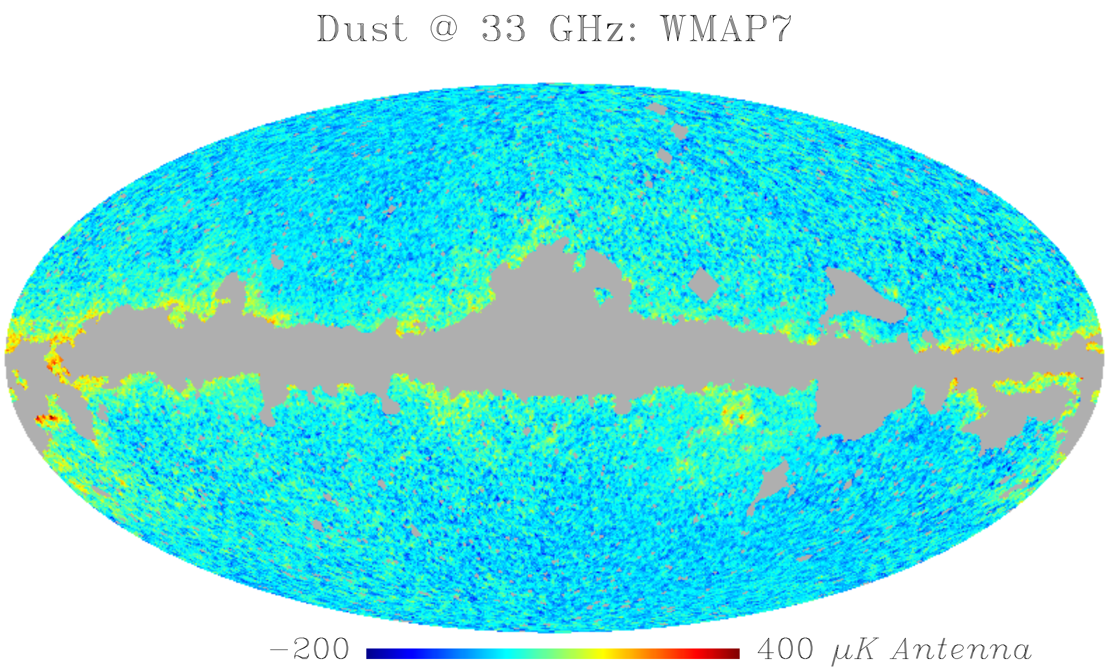

FDS model @ 94 GHz

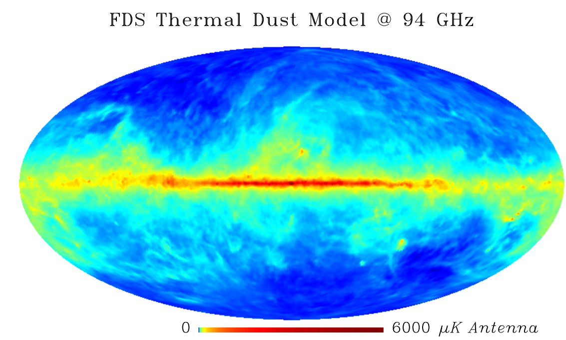

Residuals

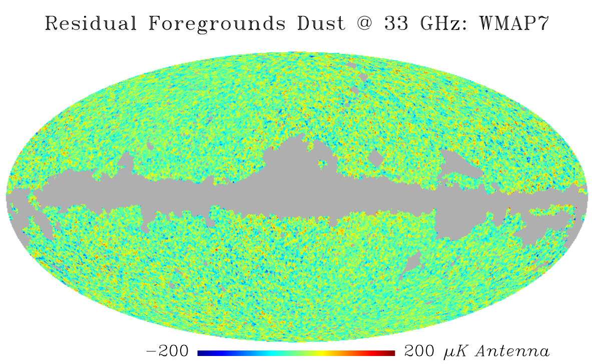

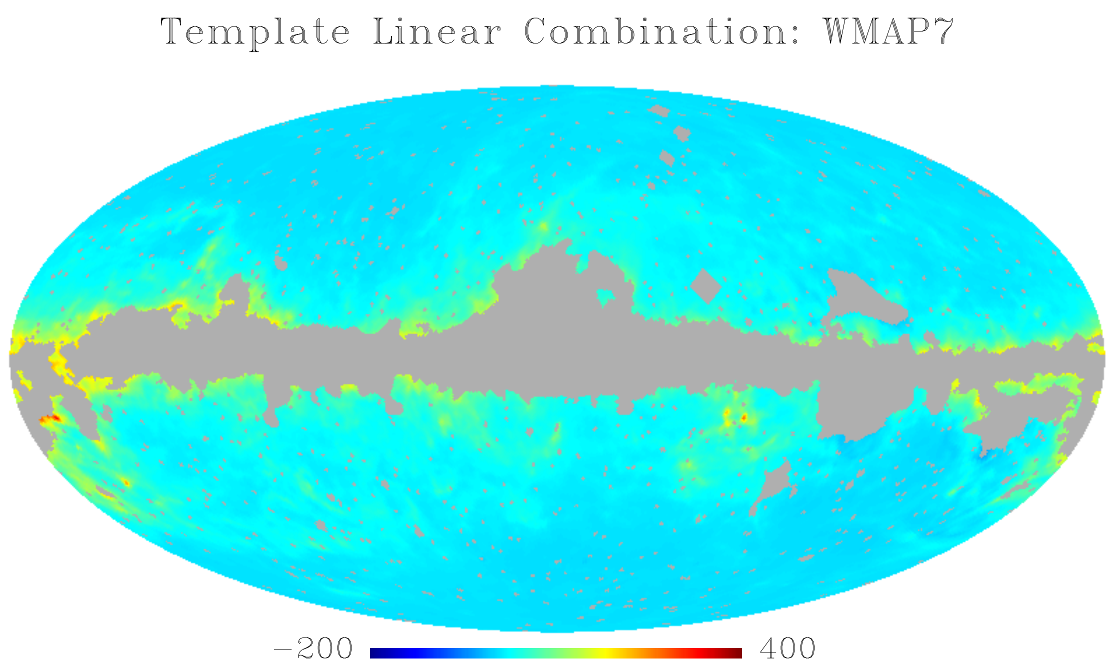

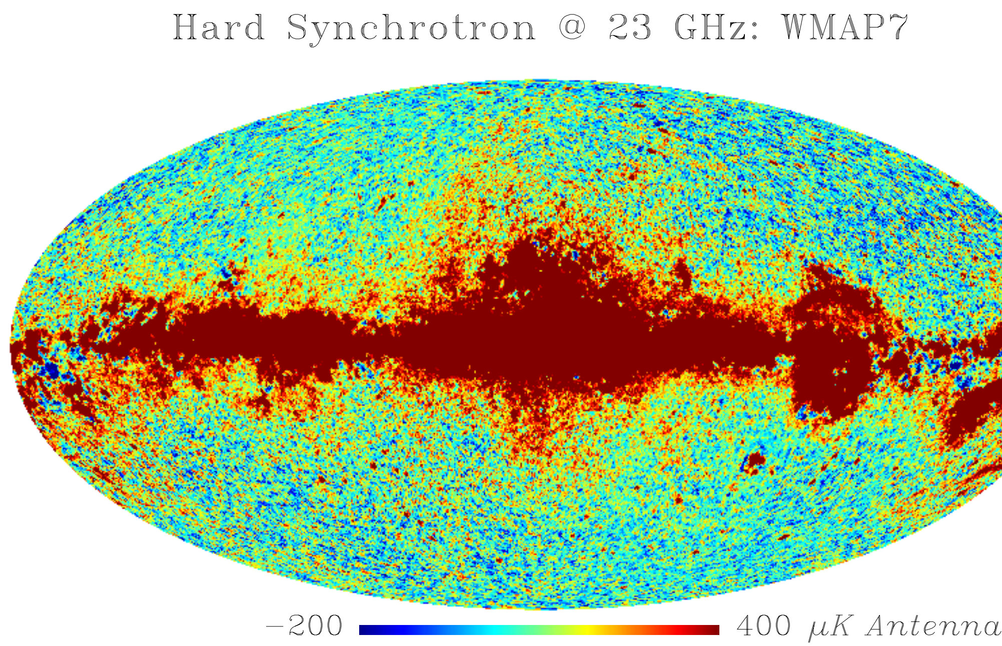

H_α or free-free emission

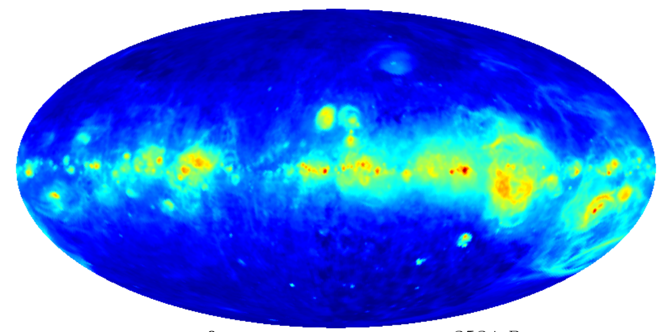

Synchrotron emission 408 MHz

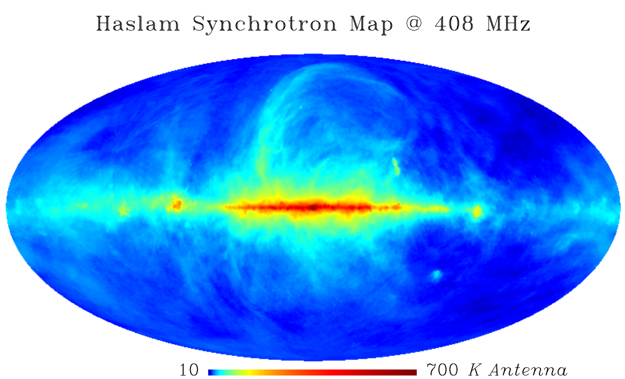

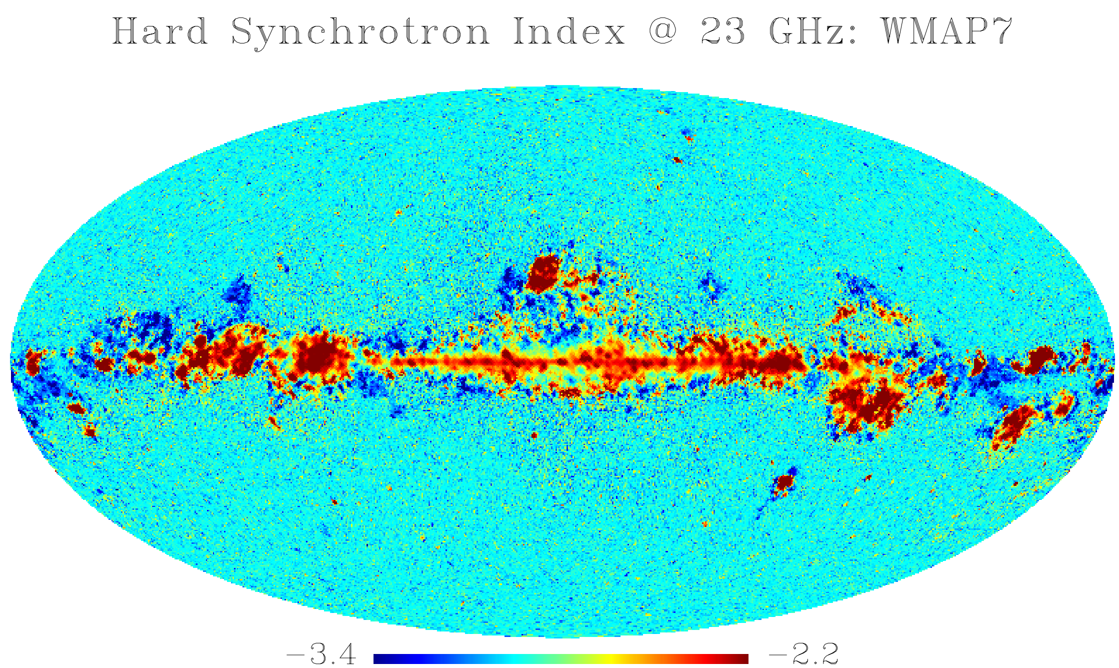

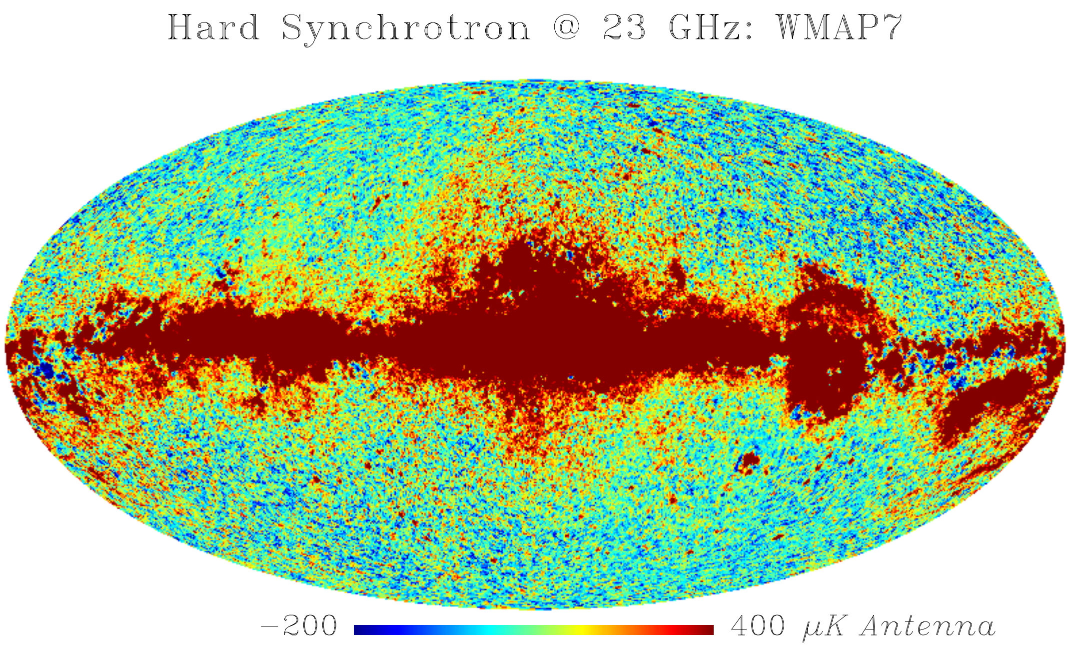

H_α or free-free emission

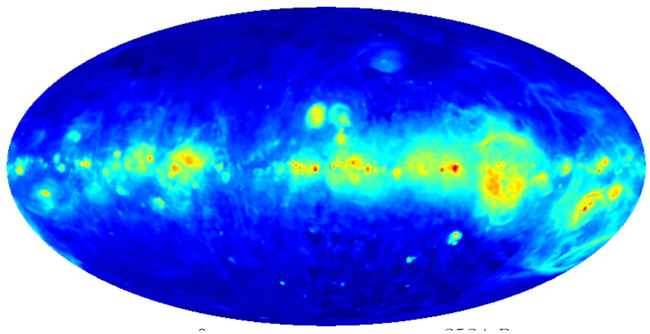

Synchrotron emission 408 MHz

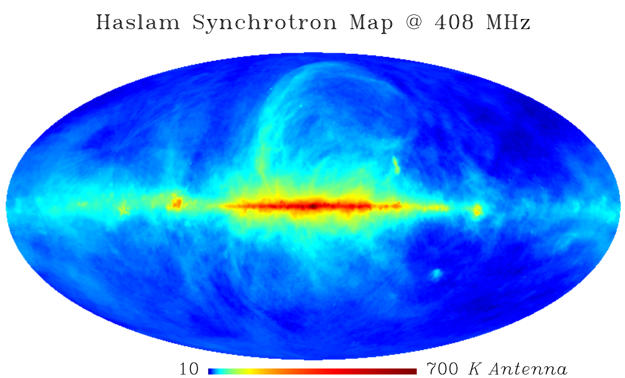

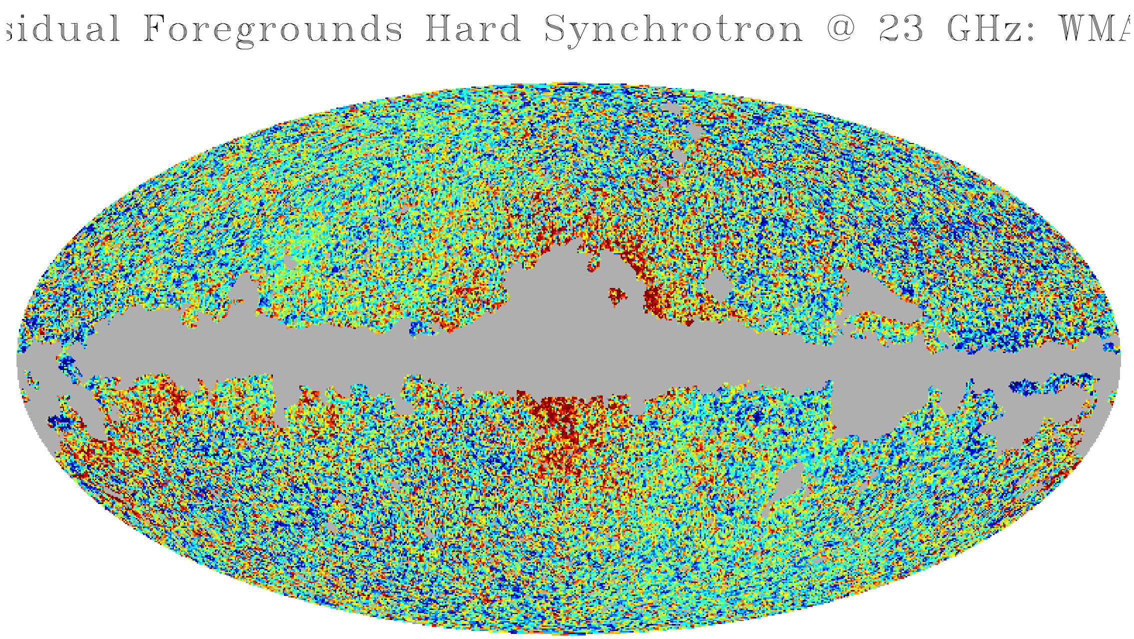

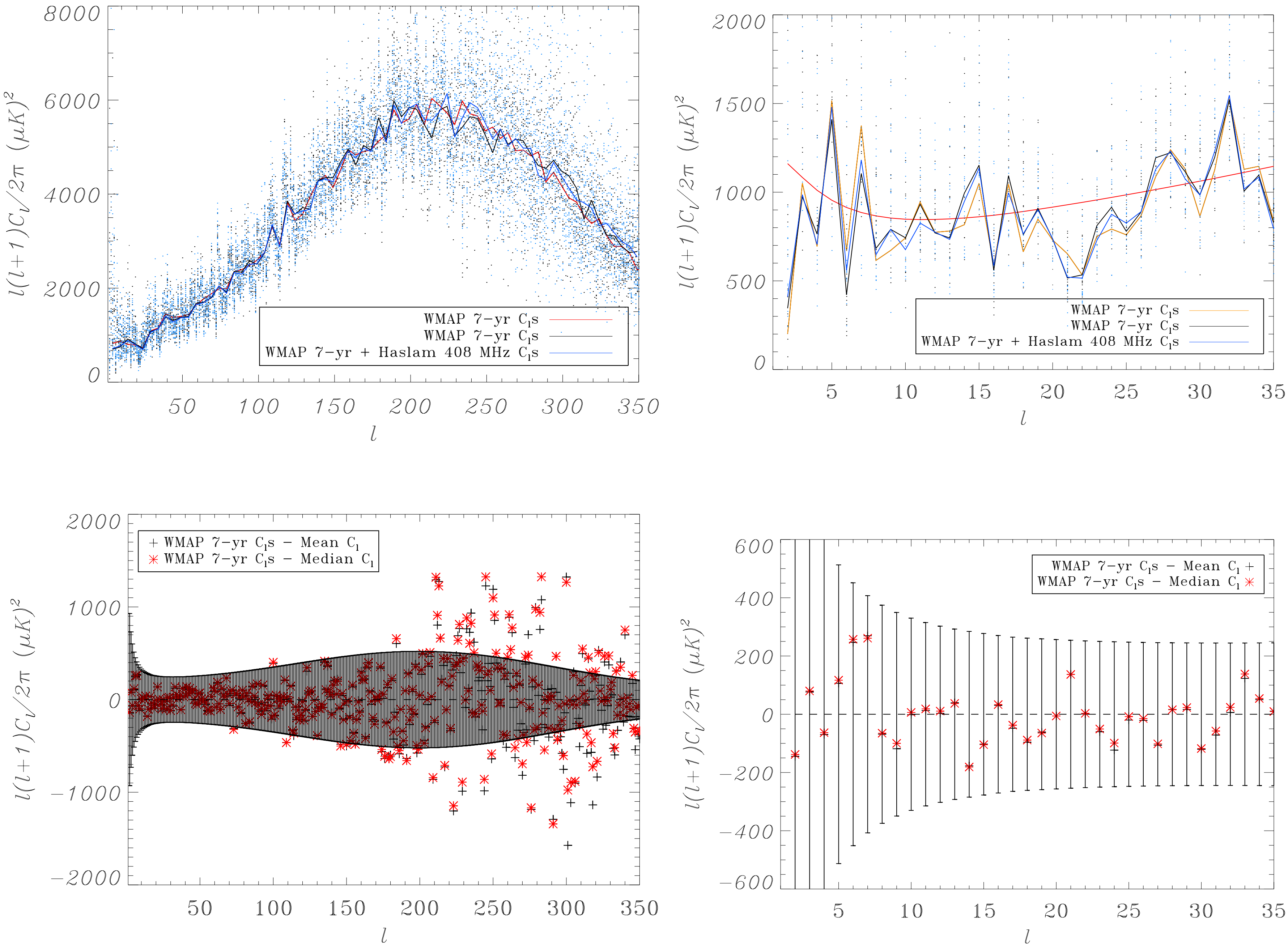

WMAP 7-yr C_ls
WMAP 7-yr C_ls
WMAP 7-yr + Haslam 408 MHz C_ls
WMAP 7-yr C_ls - Mean C_l
WMAP 7-yr C_ls - Median C_l
l(l+1)C_l/2π (μK)^2
l

Towards Planck

Foregrounds

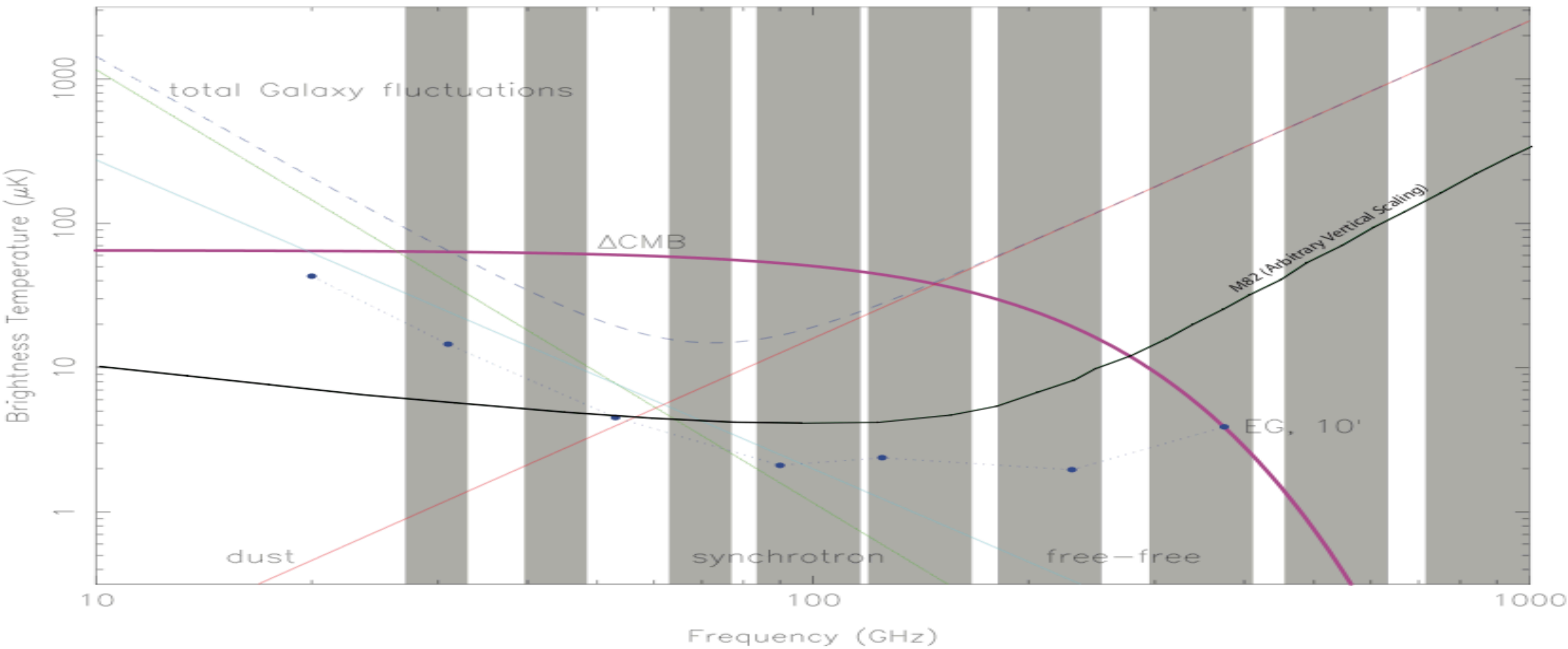

$$D(\nu) = A_d\Big(\frac{\nu}{\nu_d}\Big)^{\beta}\frac{B(\nu,T)}{B(\nu_d,T)}, \qquad \beta \simeq 1.6, T \simeq 18$$

$$S(\nu) = A_s\Big(\frac{\nu}{\nu_s}\Big)^{\alpha}, \qquad \alpha \simeq -3$$

$$f(\nu) = A_f\Big(\frac{\nu}{\nu_f}\Big)^{\epsilon}, \qquad \epsilon \simeq -2.15$$

30 GHz

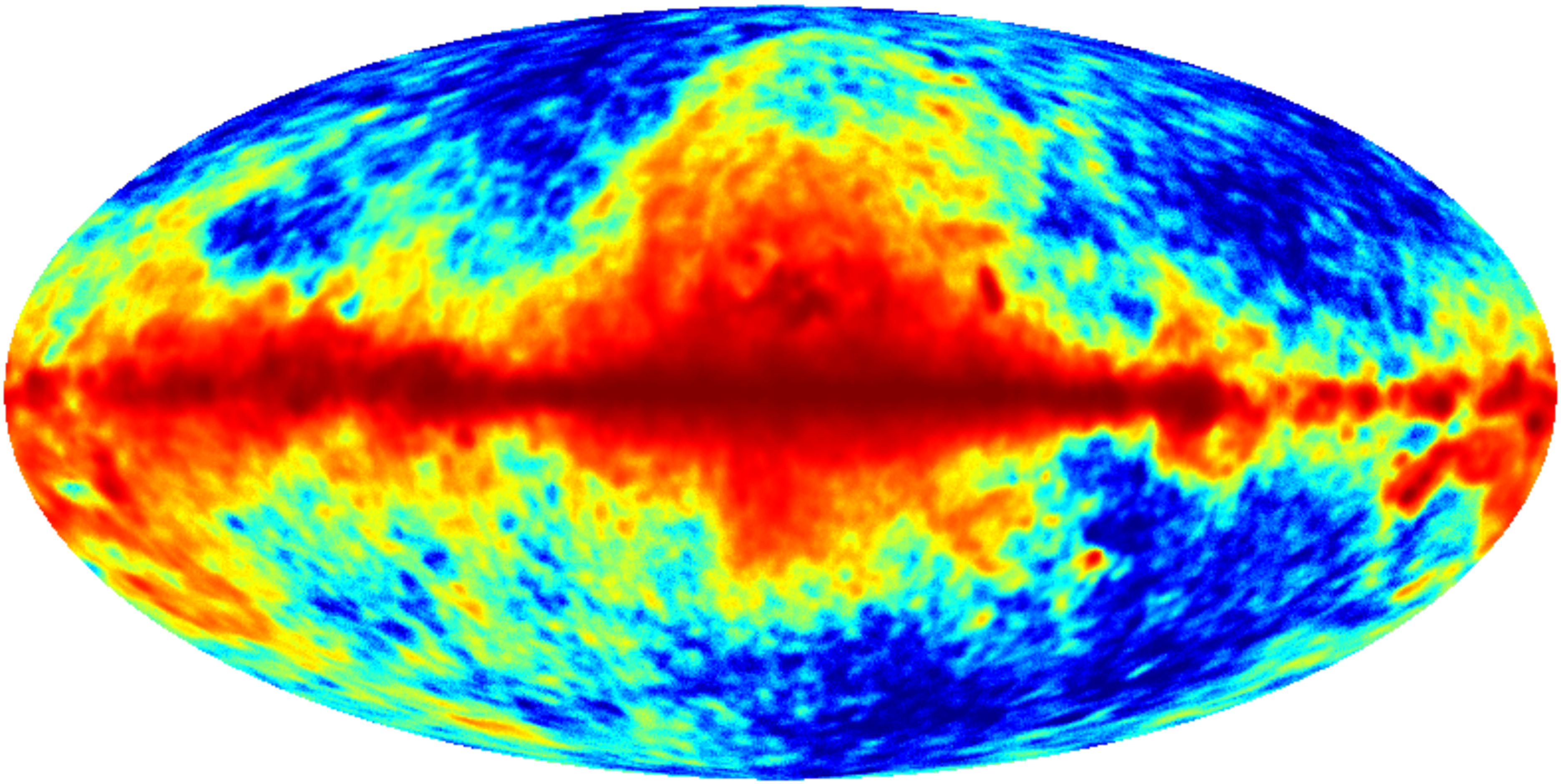

44 GHz

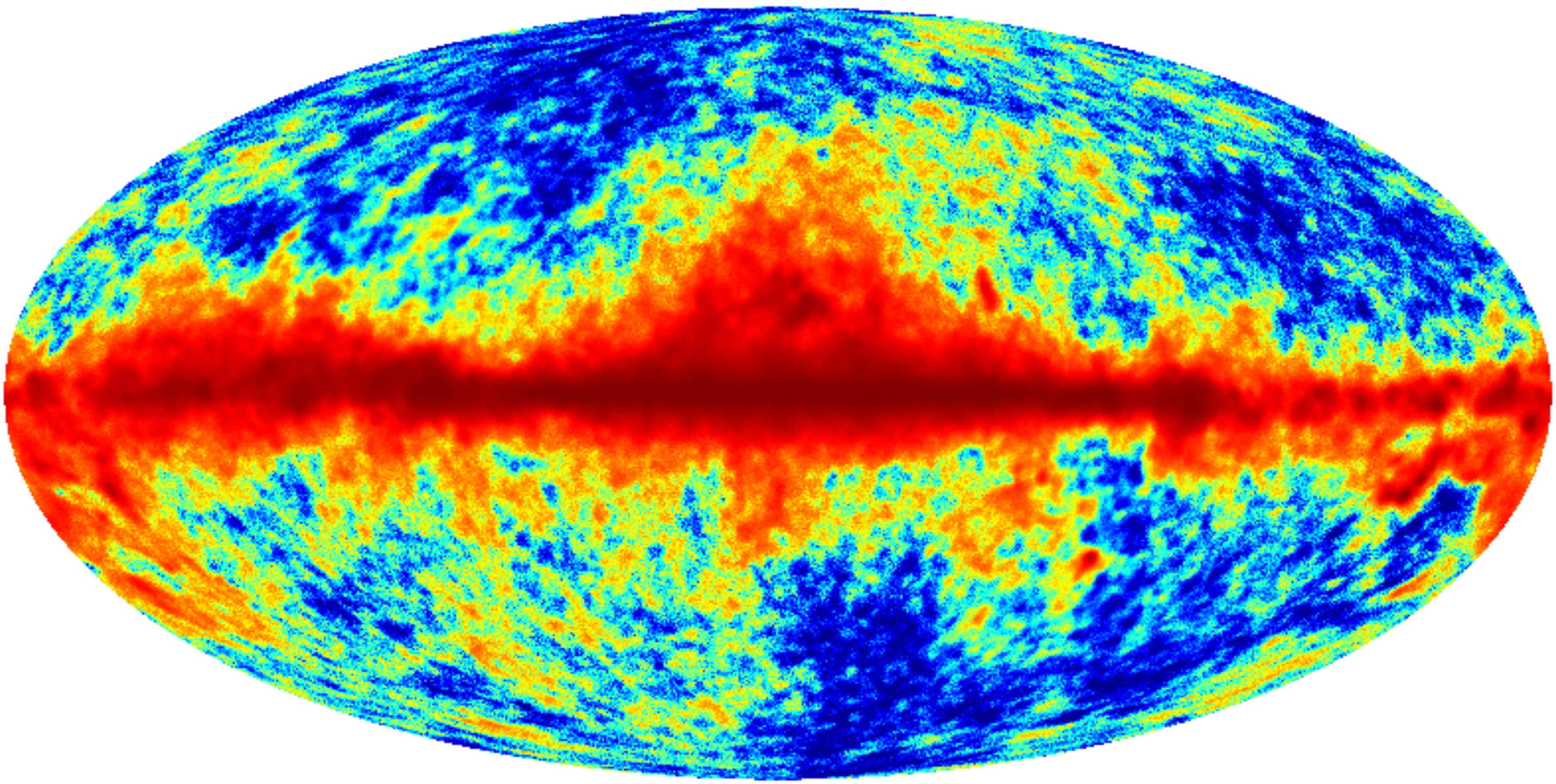

70 GHz

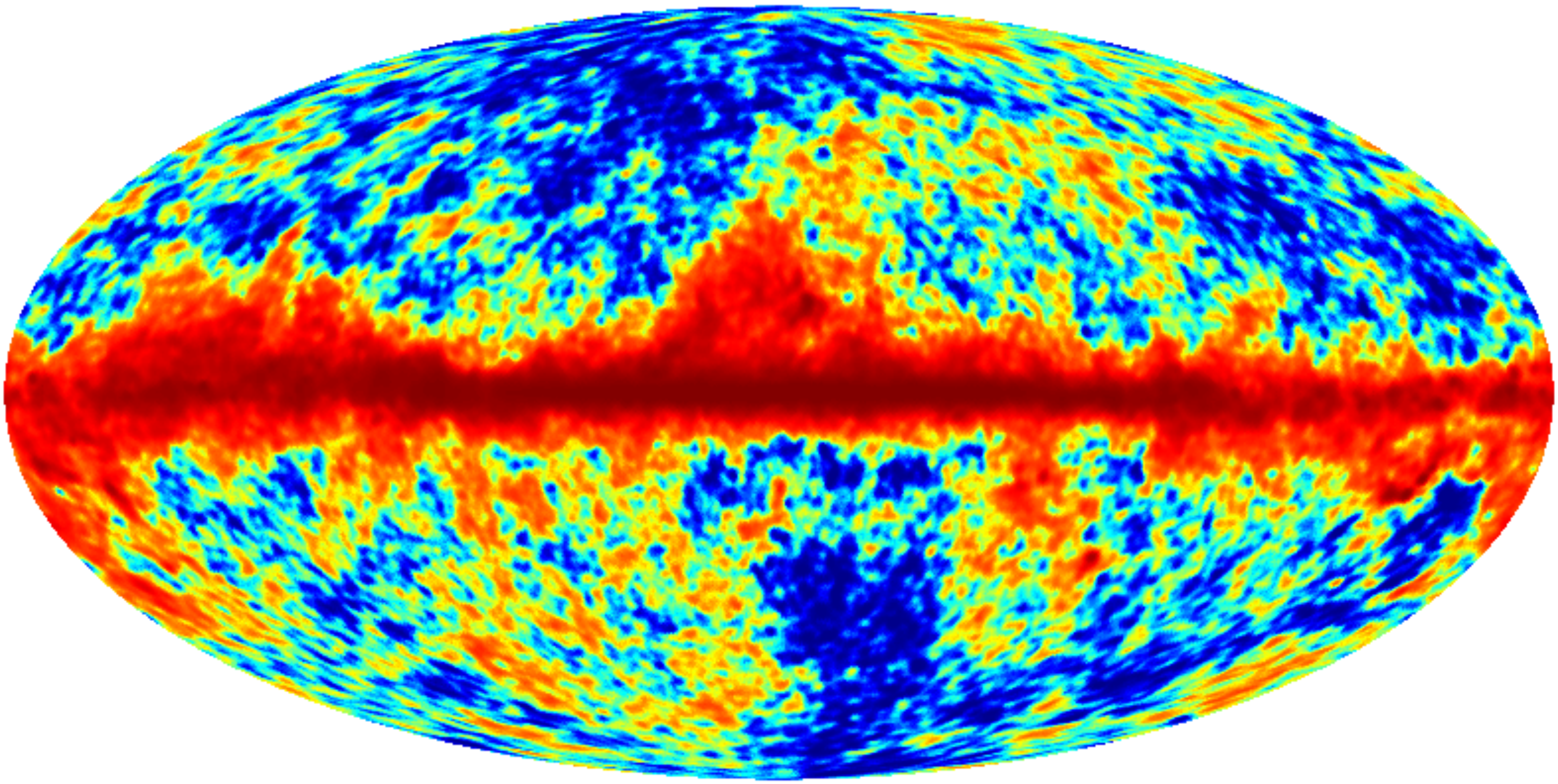

100 GHz

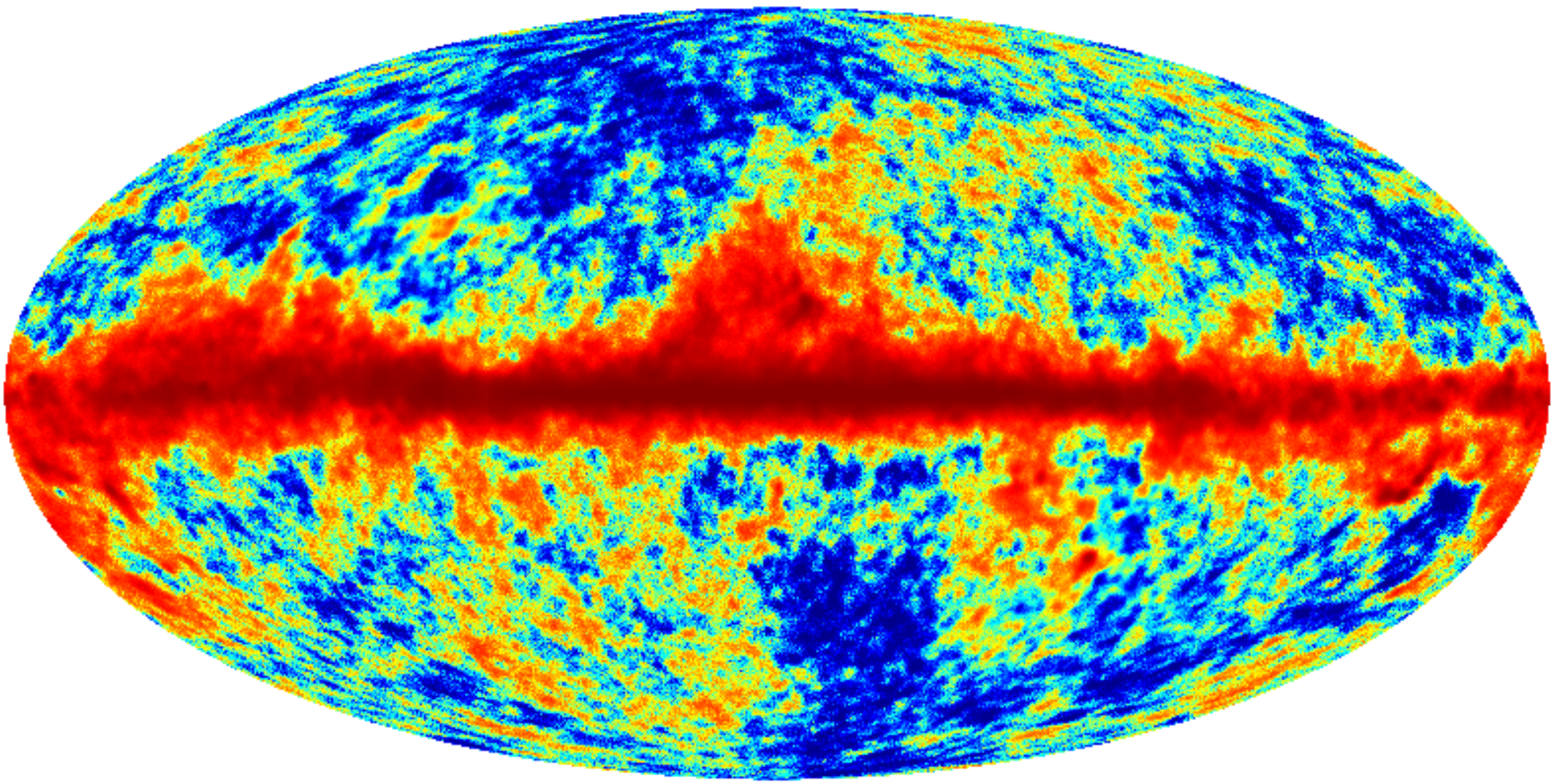

143 GHz

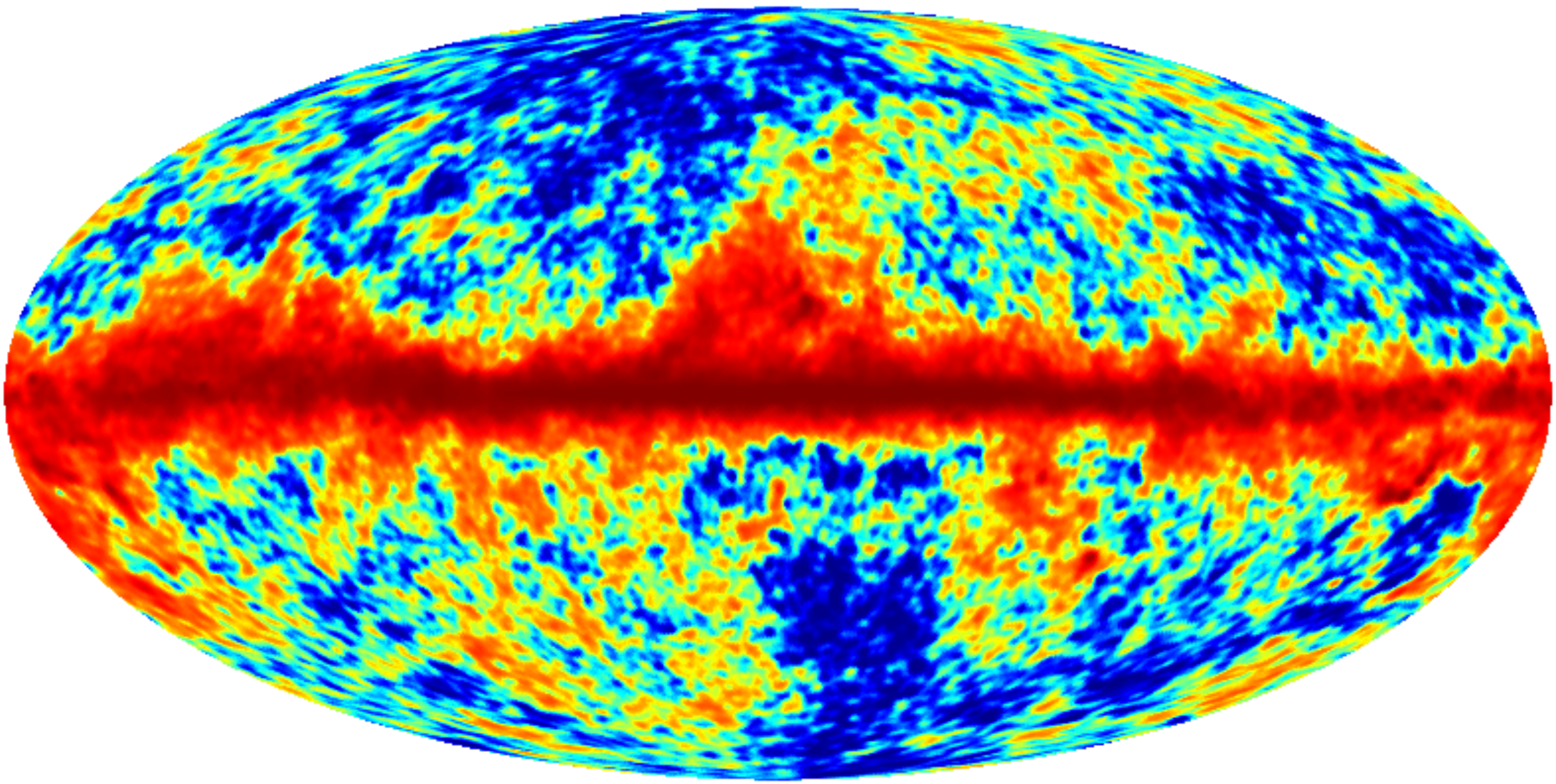

217 GHz

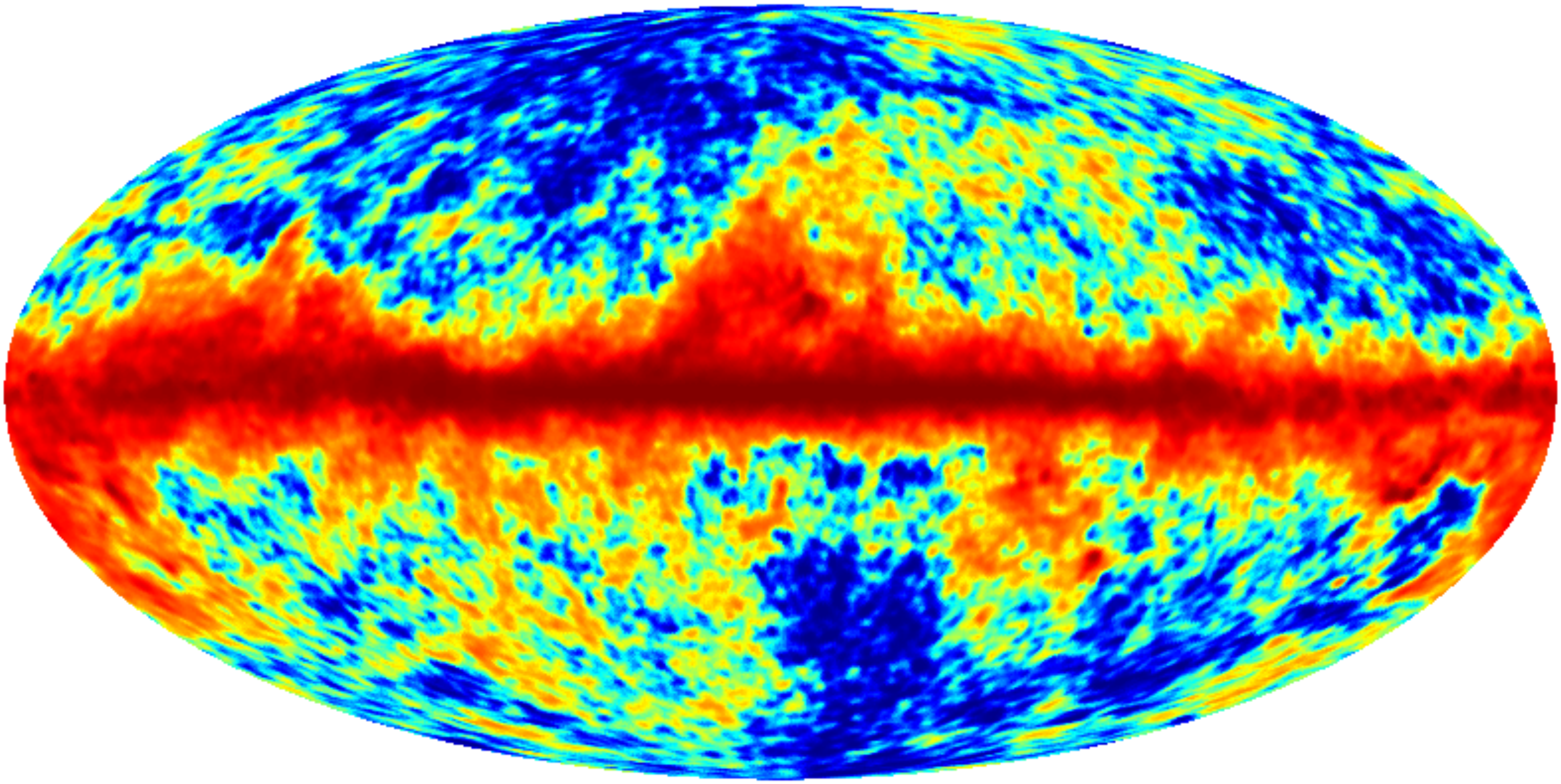

353 GHz

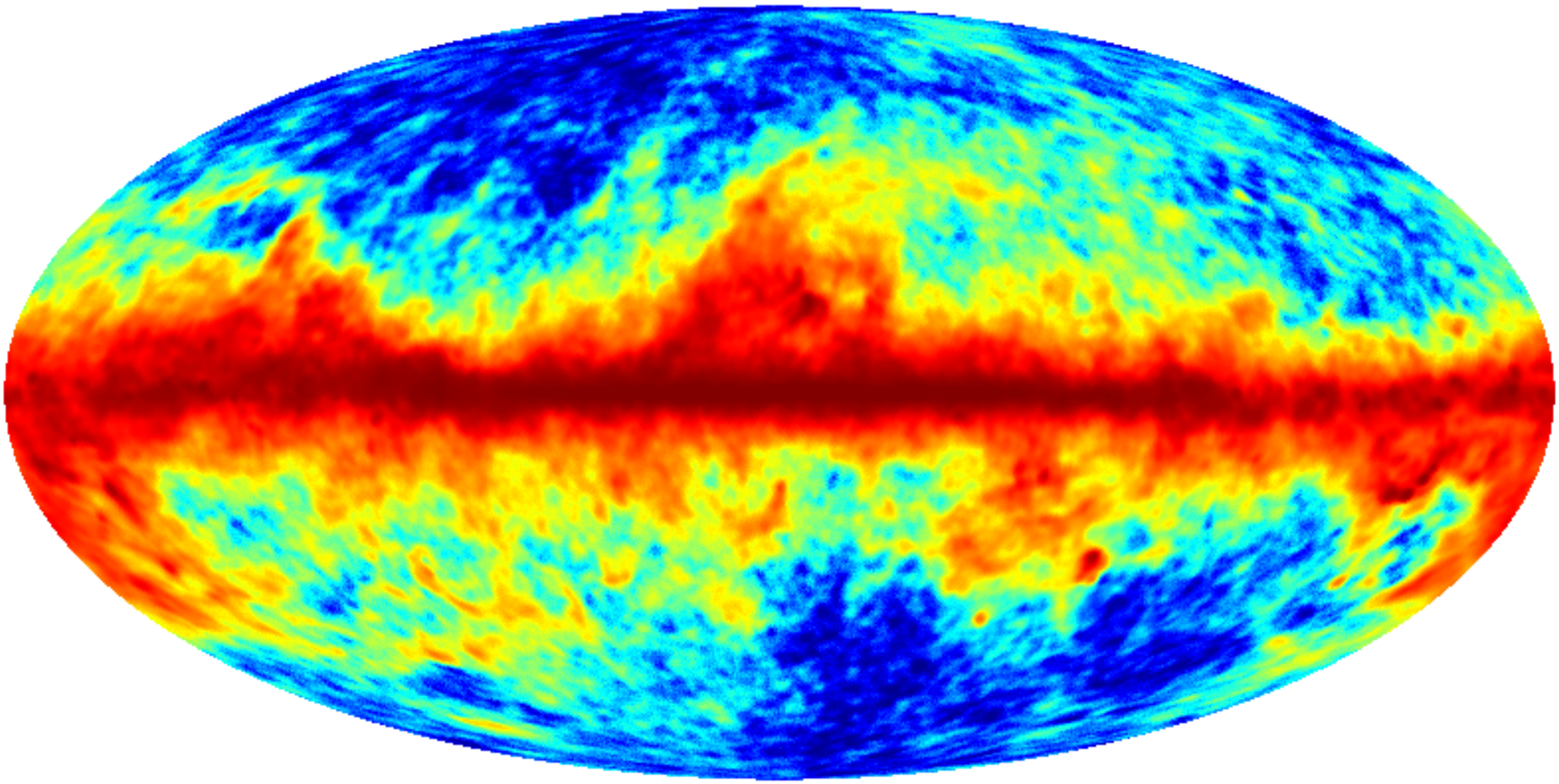

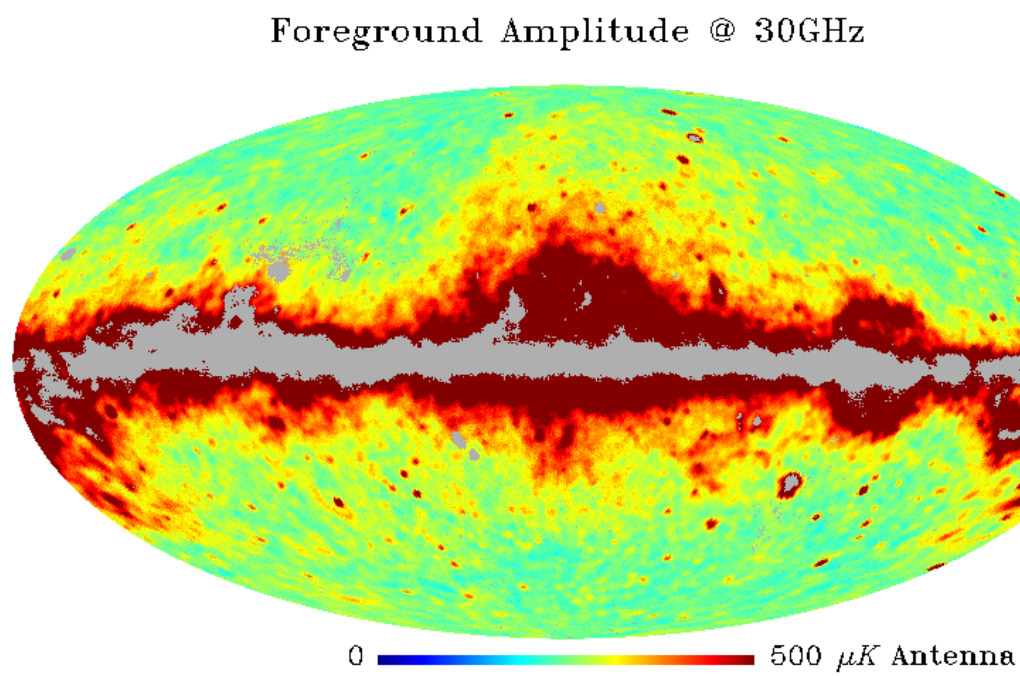
Foreground Amplitude @ 30GHz
0
500 μK Antenna

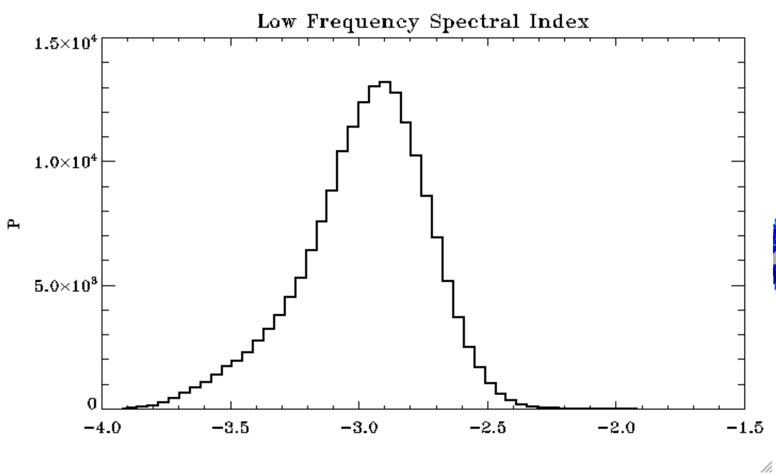
Low Frequency Spectral Index
1.5×10⁴
1.0×10⁴
5.0×10³
0
P
−4.0
−3.5
−3.0
−2.5
−2.0
−1.5

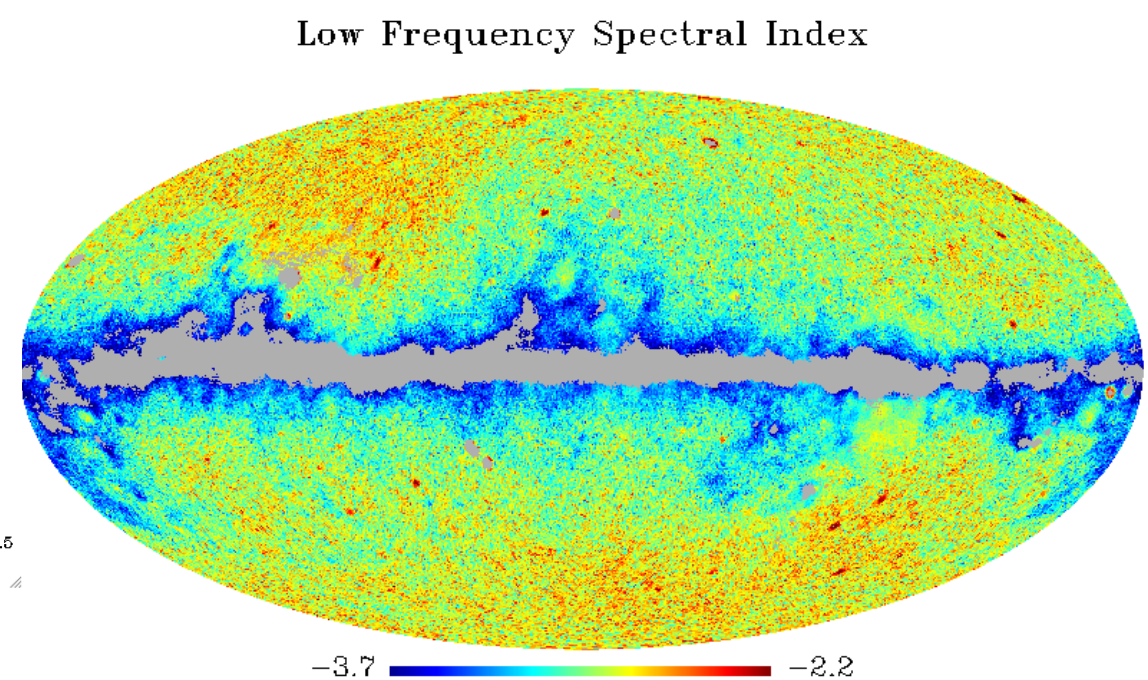
Low Frequency Spectral Index
−3.7
−2.2

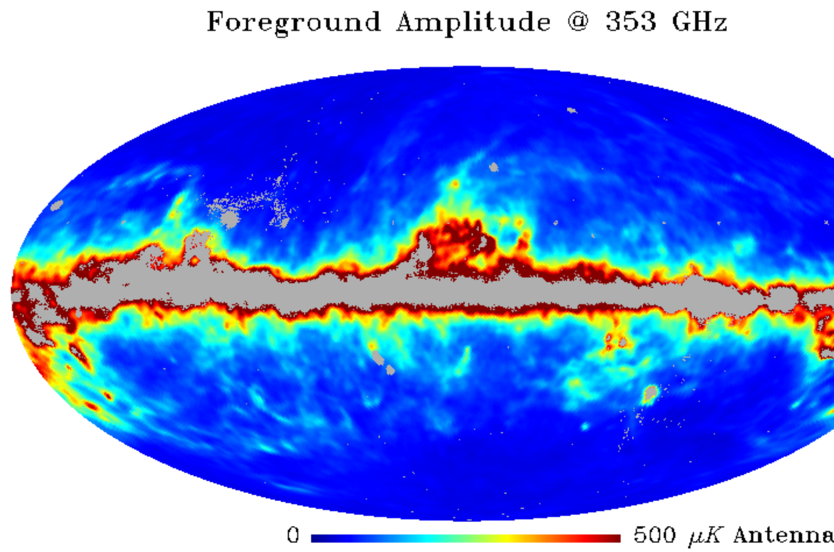
Foreground Amplitude @ 353 GHz
0
500 μK Antenna

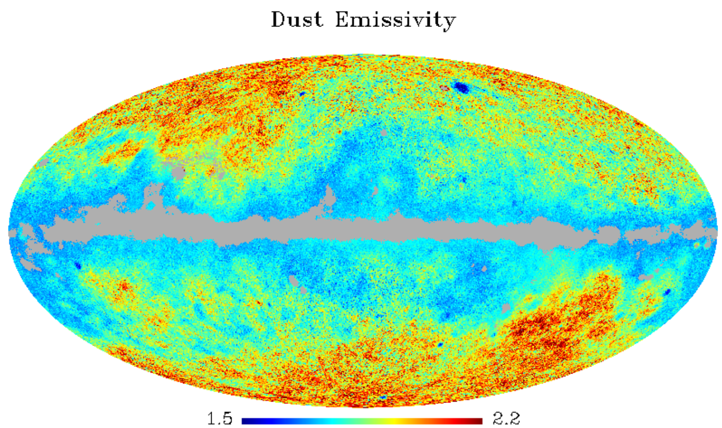
Dust Emissivity
1.5
2.2

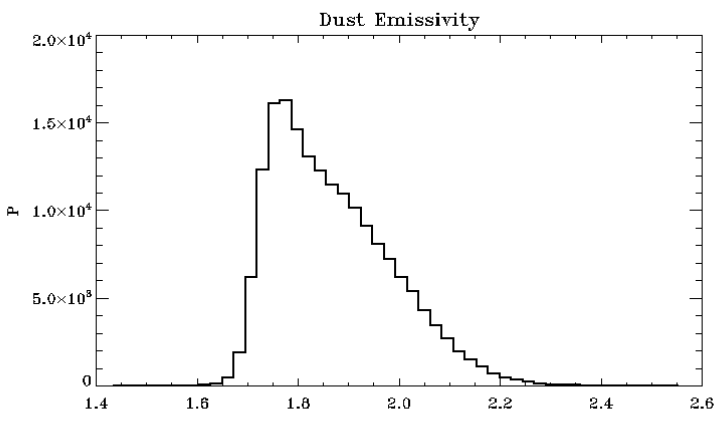
Dust Emissivity
P
2.0×10⁴
1.5×10⁴
1.0×10⁴
5.0×10³
0
1.4
1.6
1.8
2.0
2.2
2.4
2.6

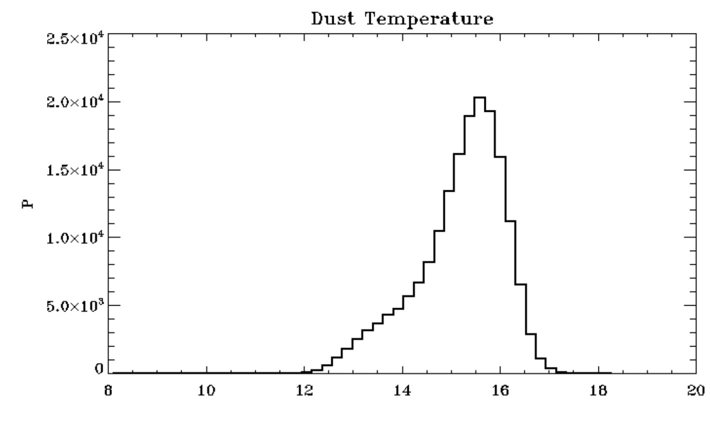
Dust Temperature
P
2.5×10⁴
2.0×10⁴
1.5×10⁴
1.0×10⁴
5.0×10³
0
8
10
12
14
16
18
20

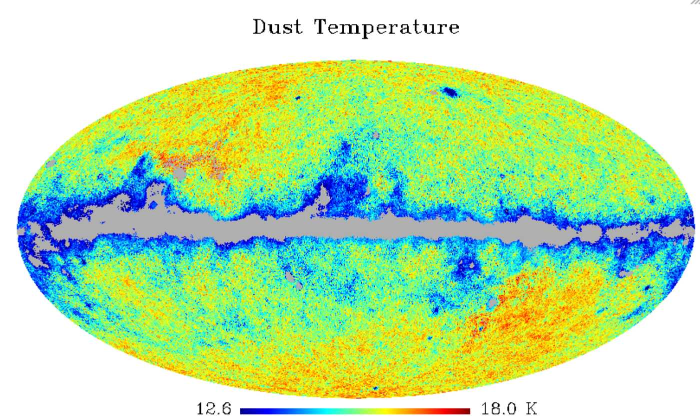
Dust Temperature
12.6
18.0 K

CMB Posterior Average

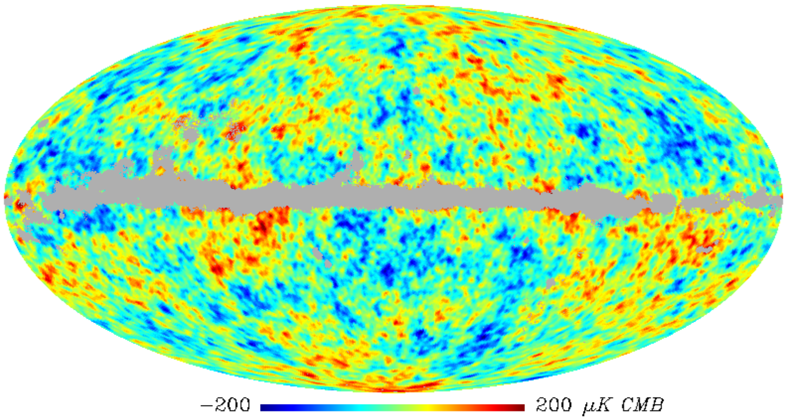

Input CMB map

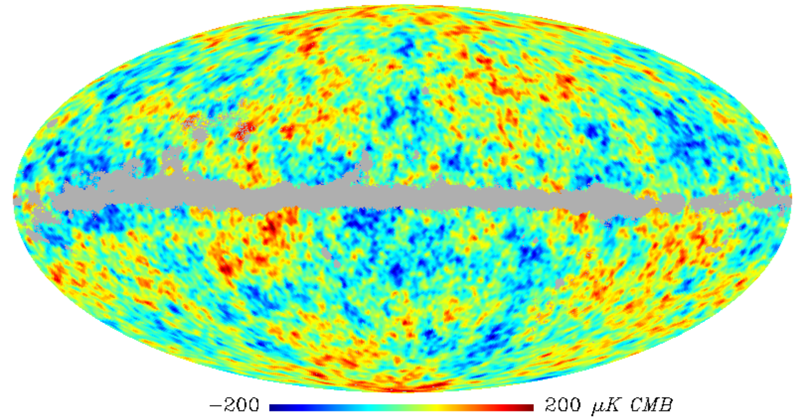

Input CMB map − Posterior Average

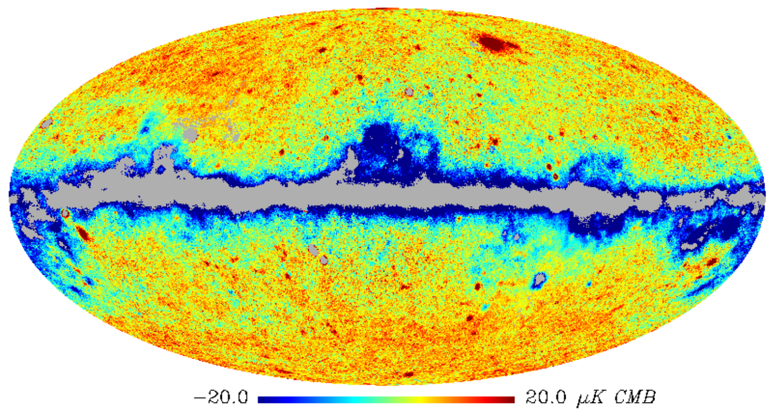

CMB RMS

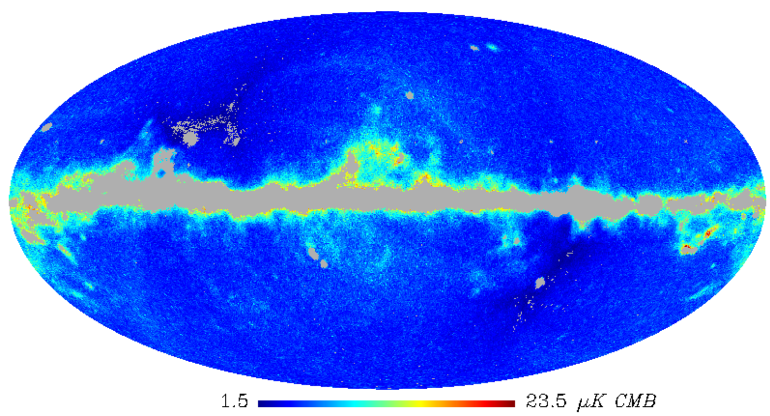

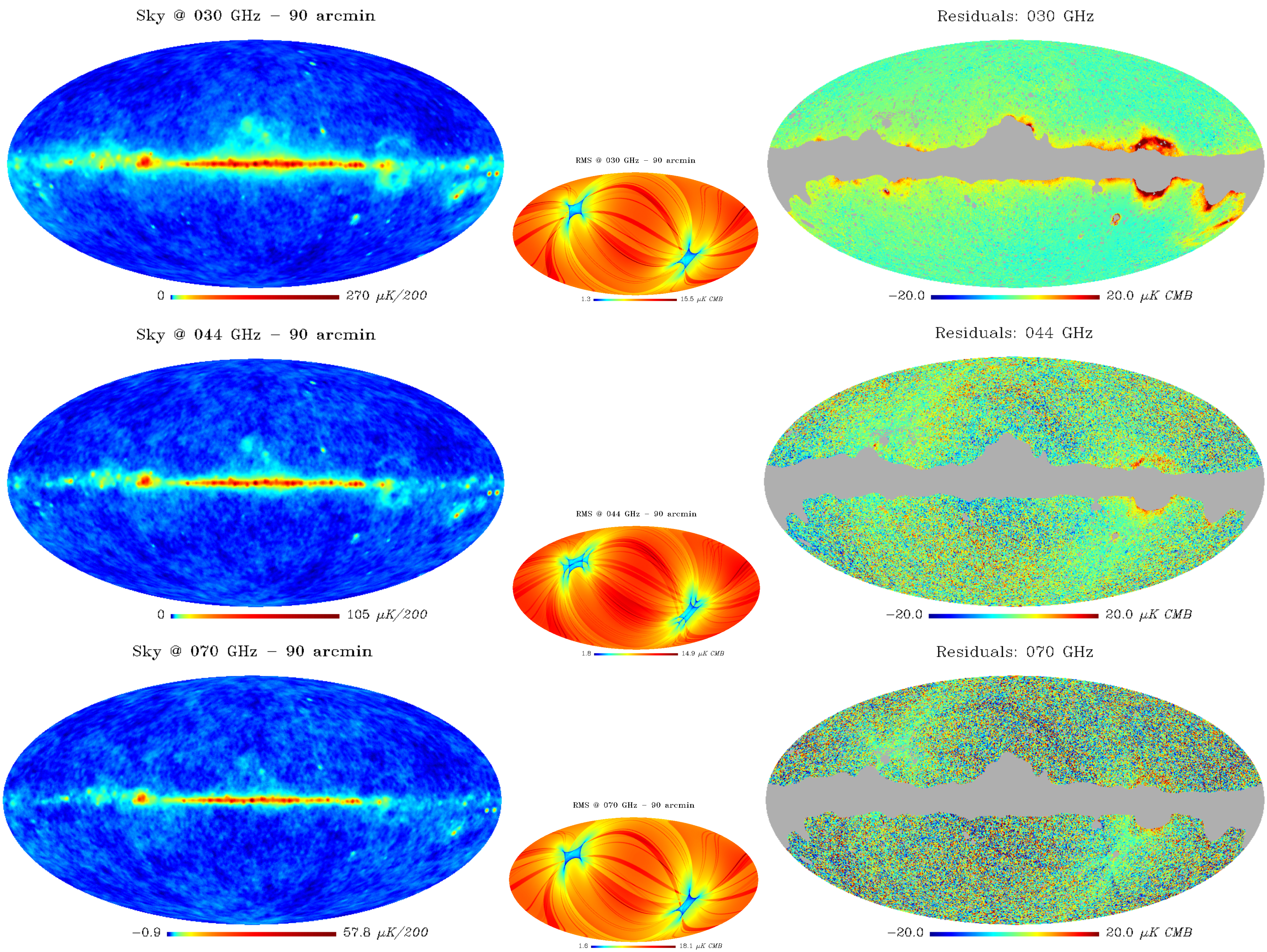

Sky @ 030 GHz – 90 arcmin
0
270 μK/200
RMS @ 030 GHz – 90 arcmin
1.3
15.5 μK CMB
Residuals: 030 GHz
−20.0
20.0 μK CMB
Sky @ 044 GHz – 90 arcmin
0
105 μK/200
RMS @ 044 GHz – 90 arcmin
1.8
14.9 μK CMB
Residuals: 044 GHz
−20.0
20.0 μK CMB
Sky @ 070 GHz – 90 arcmin
−0.9
57.8 μK/200
RMS @ 070 GHz – 90 arcmin
1.6
18.1 μK CMB
Residuals: 070 GHz
−20.0
20.0 μK CMB

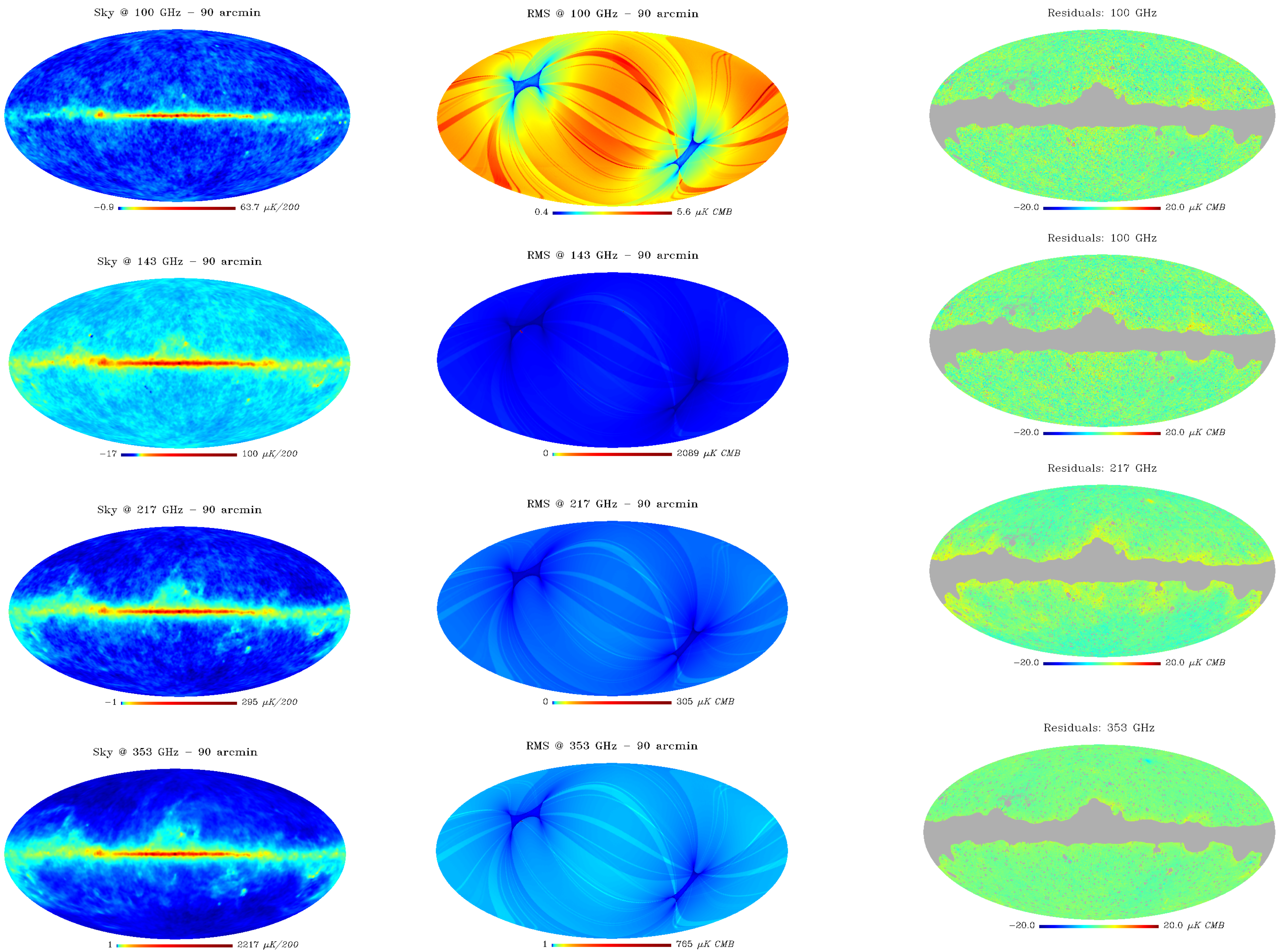
Sky @ 100 GHz − 90 arcmin
−0.9
63.7 μK/200
RMS @ 100 GHz − 90 arcmin
0.4
5.6 μK CMB
Residuals: 100 GHz
−20.0
20.0 μK CMB
Sky @ 143 GHz − 90 arcmin
−17
100 μK/200
RMS @ 143 GHz − 90 arcmin
0
2089 μK CMB
Residuals: 100 GHz
−20.0
20.0 μK CMB
Sky @ 217 GHz − 90 arcmin
−1
295 μK/200
RMS @ 217 GHz − 90 arcmin
0
305 μK CMB
Residuals: 217 GHz
−20.0
20.0 μK CMB
Sky @ 353 GHz − 90 arcmin
1
2217 μK/200
RMS @ 353 GHz − 90 arcmin
1
765 μK CMB
Residuals: 353 GHz
−20.0
20.0 μK CMB

Power law VS Gray body model for Dust

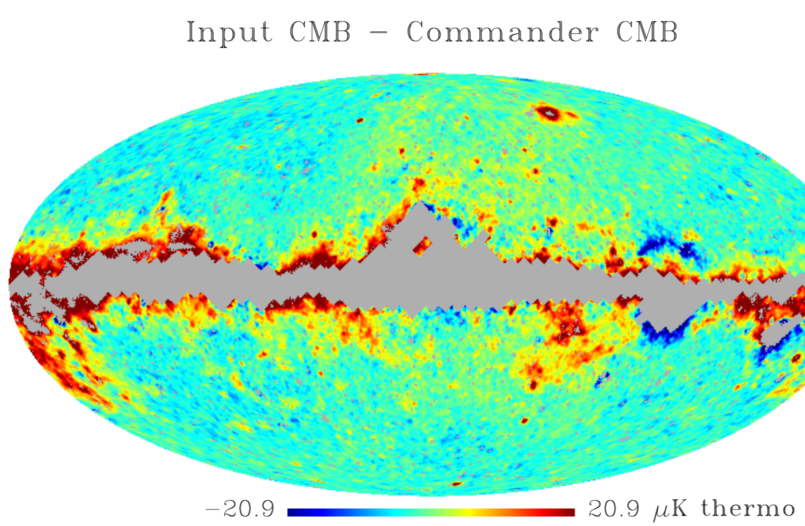

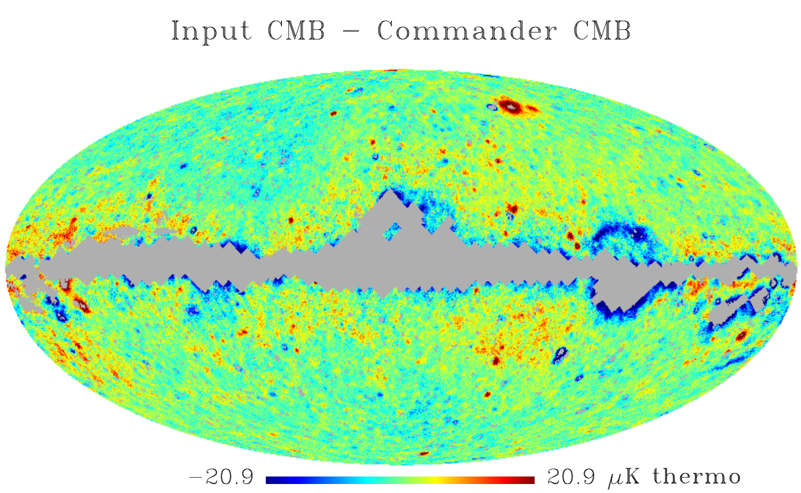

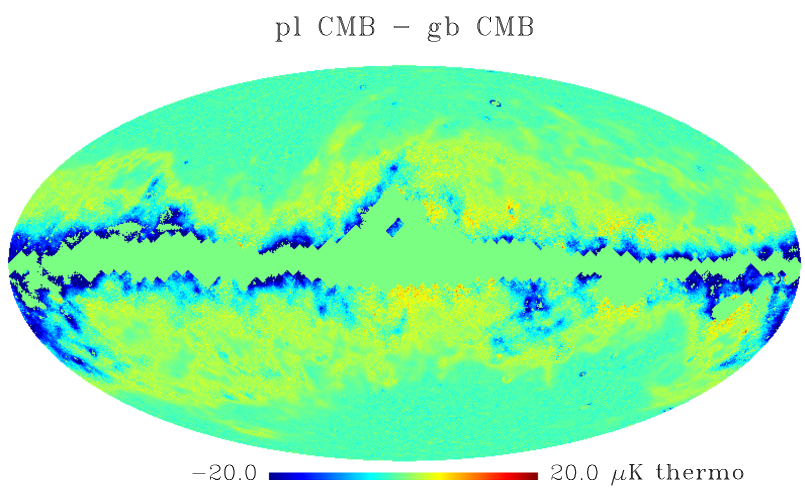

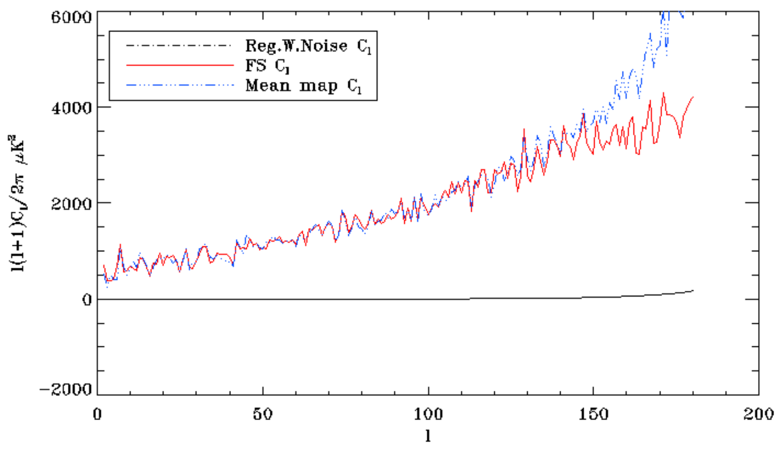

Conclusions

- Data compression based on assumptions;
- Gibbs sampling technique is extremely powerful;
    - Bayesian approach;
    - Full posterior distribution;
    - Model comparison.
- Joint Foregrounds-CMB analysis:
    - CMB map;
    - Angular power spectrum;
    - Foreground physics;
    - Full propagation of uncertainty.
- Very promising tool for Planck, well tested on WMAP